

Mathematical Models and Methods in Applied Sciences

© World Scientific Publishing Company

WULFF SHAPE EMERGENCE IN GRAPHENE

Elisa Davoli

*Faculty of Mathematics, University of Vienna, Oskar-Morgenstern-Platz 1,
A-1090 Vienna, Austria
elisa.davoli@univie.ac.at*

Paolo Piovano

*Faculty of Mathematics, University of Vienna, Oskar-Morgenstern-Platz 1,
A-1090 Vienna, Austria
paolo.piovano@univie.ac.at*

Ulisse Stefanelli

*Faculty of Mathematics, University of Vienna, Oskar-Morgenstern-Platz 1,
A-1090 Vienna, Austria,
and Istituto di Matematica Applicata e Tecnologie Informatiche "E. Magenes" - CNR,
v. Ferrata 1, I - 27100 Pavia, Italy
ulisse.stefanelli@univie.ac.at*

Received (Day Month Year)

Revised (Day Month Year)

Communicated by (xxxxxxxxxx)

Graphene samples are identified as minimizers of configurational energies featuring both two- and three-body atomic-interaction terms. This variational viewpoint allows for a detailed description of ground-state geometries as connected subsets of a regular hexagonal lattice. We investigate here how these geometries evolve as the number n of carbon atoms in the graphene sample increases. By means of an equivalent characterization of minimality via a discrete isoperimetric inequality, we prove that ground states converge to the ideal hexagonal Wulff shape as $n \rightarrow \infty$. Precisely, ground states deviate from such hexagonal Wulff shape by at most $Kn^{3/4} + o(n^{3/4})$ atoms, where both the constant K and the rate $n^{3/4}$ are sharp.

Keywords: Ground state, hexagonal lattice, isoperimetric inequality, Wulff shape.

AMS Subject Classification: 82D25.

2 *Elisa Davoli, Paolo Piovano, and Ulisse Stefanelli*

1. Introduction

The recent realization of high crystalline quality graphene samples at room temperature can be regarded as a breakthrough in Materials Science and has led to the attribution of the 2010 Nobel Prize in Physics to Geim and Novoselov. The fascinating electronic and mechanical properties of single-atom-thick carbon surfaces are believed to offer unprecedented opportunities for innovative applications, ranging from next-generation electronics to pharmacology, and including batteries and solar cells. New findings are emerging at an always increasing pace and involve thousands of researchers worldwide cutting across Materials Science, Physics, and Chemistry, extending from fundamental science to novel applications.

The stand of the mathematical understanding of graphene is comparably less developed. All available results are extremely recent and concern the modeling of transport properties of electrons in graphene sheets, ^{3,6,13,16,25,34,35} homogenization, ^{8,33} atomistic-to-continuum passage for nanotubes, ¹⁴ geometry of monolayers under Gaussian perturbations, ¹¹ external charges ²⁷ or magnetic fields, ¹⁰ combinatorial description of graphene patches, ²² and numerical simulation of dynamics via nonlocal elasticity theory. ⁴⁴ Remarkably, the determination of the equilibrium shapes and the Wulff shapes of graphene samples and graphene nanostructures is still a challenging problem. ^{1,5,19}

Graphene ideally corresponds to a regular, two-dimensional, hexagonal arrangement of carbon atoms. In the bulk of a graphene sample each carbon atom is covalently bonded to three neighbors. These covalent bonds are of sp^2 -hybridized type and ideally form $2\pi/3$ angles in a plane. In order to describe these bonds, some phenomenological interaction energies, including two- and three-body interaction terms, have been presented and partially validated. ^{38,39} The arrangement of carbon atoms in the two-dimensional crystal emerges then as the global effect of the combination of local atomic interactions, and can be seen as the result of a *geometric optimization* process: by identifying the *configuration* of n carbon atoms with their positions $\{x_1, \dots, x_n\} \subset \mathbb{R}^2$, one minimizes a given *configurational energy* $E : \mathbb{R}^{2n} \rightarrow \mathbb{R} \cup \{\infty\}$ and proves that the minimizers are indeed subsets of a regular hexagonal lattice. The configurational energies for carbon feature a decomposition $E = E_2 + E_3$ where E_2 corresponds to an attractive-repulsive two-body interaction, favouring some preferred spacing of the atoms, and E_3 encodes three-body interactions, expressing the specific geometry of sp^2 -covalent bonding in carbon.

The above variational viewpoint brings the study of graphene geometries into the realm of the so-called *crystallization problems*. A first analysis in this direction is in Ref. ¹², where E_2 is assumed to be of Lennard-Jones type and E_3 favors $2\pi/3$ and $4\pi/3$ bond angles. The focus of Ref. ¹² is on the *thermodynamic limit*: as $n \rightarrow \infty$ the minimal energy density is proven to converge to a finite value, corresponding indeed to the configuration in which the atoms arrange themselves in a suitably stretched

hexagonal lattice. Analogous thermodynamic-limit results are obtained in Ref. 15, where nonetheless the term E_2 favors π bond angles. The crystallization problem for a *finite number* of carbon atoms is studied in Ref. 32 where the periodicity of ground states as well as the exact quantification of the ground-state energy is obtained, together with the discussion of carbon nanostructures such as fullerenes and nanotubes, see also Refs. 28, 29, 32. The reader is referred to Refs. 20, 41, 42 for one-dimensional crystallization results, to Refs. 24, 36, 43 and Ref. 40 in the two-dimensional case either in the finite and in the thermodynamic-limit case, and to Refs. 30, 31 for crystallization in the square lattice. Results on the three-dimensional thermodynamic limit are available in Refs. 17, 18, and a recent review on the crystallization problem can be found in Ref. 4.

Our analysis moves from the consideration that, as the configurational energy favors bonding, ground states are expected to have minimal perimeter, since boundary atoms have necessarily less neighbors. These heuristics are here made precise by providing a new characterization of ground states based on a crystalline isoperimetric inequality. Indeed, we prove in Proposition 3.4 below that ground states correspond to isoperimetric extremizers and we determine the exact isoperimetric constant. Analogous results are obtained in Refs. 30, 31 for the square lattice, and in Ref. 9 for the triangular lattice.

The minimality of the ground-state perimeter gives rise to the emergence of large polygonal clusters as the number of atoms n increases. Indeed, one is interested in identifying a so-called *Wulff shape* to which all properly rescaled ground states converge. This has been successfully obtained for both the triangular 2,9,37 and the square lattice, 30,31 where ground states approach a hexagon and a square, respectively, as $n \rightarrow \infty$. Quite remarkably, in both the triangular and the square case it has been proved that ground states differ from the Wulff shape by at most $O(n^{3/4})$ atoms, this bound being sharp. This is what it is usually referred to as the $n^{3/4}$ -law.

The central aim of this paper is to establish the Wulff shape emergence for graphene samples and to investigate the $n^{3/4}$ -law in this setting. Precisely, we provide sharp quantitative convergence results for ground states G_n to the correspondingly rescaled Wulff shape, in terms both of the Hausdorff distance and of the flat distance of the empirical measures μ_{G_n} , to the measure with density $\frac{4}{\sqrt{3}}\chi_W$, i.e. the rescaled characteristic function of the (rescaled) hexagonal Wulff shape.

With respect to previous contributions to this subject the novelty of our paper is threefold. First, we provide a complete characterization of ground states, for all numbers of atoms, as well as a detailed description of their geometry. In particular, as a byproduct of our isoperimetric characterization we are able to investigate the edge geometry of graphene patches. Graphene atoms tend to naturally arrange themselves into *hexagonal samples* whose edges can have, roughly speaking, two shapes: they can either form *zigzag* or *armchair* structures (see Refs. 5, 21, 26 and

4 *Elisa Davoli, Paolo Piovano, and Ulisse Stefanelli*

below)).

We prove here that hexagonal configurations having armchair edges do not satisfy the isoperimetric equality, whereas those with zigzag edges do (see Definition 4.1). Namely, we have the following.

Theorem 1.1 (Zigzag-edge selectivity). *Zigzag hexagons are ground states, armchair hexagons are not.*

This provides an analytical counterpart to the experimental results in Ref. 26, confirming the zigzag-edge selectivity in the growth process of graphene samples.

The second main result of the paper is the discussion of the Wulff shape emergence in the hexagonal system, which is not a simple Bravais lattice but rather a so-called multilattice. We relate the Wulff shape emergence with the isoperimetric nature of ground states. Our result reads as follows.

Theorem 1.2 (Emergence of the Wulff shape). *Let G_n be a sequence of ground states in the hexagonal lattice. Let W_n be the zigzag hexagon centered in the origin and with side r_n (see (1.6) below). Then, there exists a suitable translation G'_n of G_n such that*

$$|G'_n \setminus W_n| \leq Kn^{3/4} + o(n^{3/4}), \quad (1.1)$$

where $|\cdot|$ is the cardinality of the set, and

$$K := \frac{2^{7/4}}{3^{1/4}}. \quad (1.2)$$

In addition, there holds

$$d_{\mathcal{H}}(G'_n, W_n) \leq O(n^{1/4}),$$

$$\|\mu_{G'_n} - \mu_{W_n}\| \leq Kn^{-1/4} + o(n^{-1/4}), \quad (1.3)$$

$$\|\mu_{G'_n} - \mu_{W_n}\|_F \leq Kn^{-1/4} + o(n^{-1/4}), \quad (1.4)$$

$$\mu_{G'_n} \rightharpoonup^* \frac{4}{\sqrt{3}}\chi_W \quad \text{weakly}^* \text{ in the sense of measures,}$$

and

$$\left\| \mu_{G'_n} - \frac{4}{\sqrt{3}}\chi_W \right\|_F \leq 2Kn^{-1/4} + o(n^{-1/4}), \quad (1.5)$$

where $d_{\mathcal{H}}$ is the Hausdorff distance, $\|\cdot\|$ is the total variation, and $\|\cdot\|_F$ is the flat norm (see (2.4)).

Our third main result concerns the sharpness of the $n^{3/4}$ -law (1.1). We show not only the sharpness of the convergence ratio, but also of the constant K in front of the leading term. We have the following.

Theorem 1.3 (Sharpness of the $n^{3/4}$ -law). *There exists a sequence of integers*

n_j such that for every sequence of ground states $\{G_{n_j}\}$ properties (1.1), (1.3), and (1.4) hold with equalities.

Our proof strategy differs from that of Refs. 30, 37, as it is not based on configuration rearrangements. The argument here moves from the control of the radius r_{G_n} of the maximal hexagon H_{G_n} contained in a ground state G_n with n atoms. In particular, we define

$$r_n := \min\{r_{G_n} : G_n \text{ is a ground state with } n \text{ atoms}\}, \quad (1.6)$$

and we show that every ground state (up to translation) consists of the n -Wulff shape W_n with comparably few extra atoms, see Section 6. Precisely, we prove a delicate estimate of the form $r_n \sim n^{1/2}$ which entails that the atoms of G_n which do not belong to W_n are at most $O(n^{3/4})$. An outcome of our proof is that the convergence rates and the constants above are sharp. Indeed, we explicitly construct a sequence of integers such that every corresponding sequence of ground states attains the right-hand sides of (1.1), (1.3), and (1.4).

In the triangular lattice, the existence of a sequence of ground states whose deviation from the Wulff shape is exactly of order $n^{3/4}$ was exhibited in Ref. 37 with no specific control on the convergence constants. With a different implementation of the method discussed here, we revisited the triangular-lattice case in Ref. 9, obtaining explicit, sharp convergence constants.

The paper is organized as follows. In Section 2 we introduce some notation and a few definitions. In Section 3 we highlight the isoperimetric nature of ground states. Section 4 contains a discussion of the equilibrium shapes of graphene samples, and a proof of the fact that *armchair hexagons* are not ground states. In particular we prove there Theorem 1.1. In Section 5 we provide delicate lower and upper bounds for r_n . Section 6 is eventually devoted to the proofs of Theorems 1.2 and 1.3.

2. Notation and Setting of the problem

Let the *hexagonal lattice* be given by

$$\mathcal{L} := \{mt_1 + nt_2 + cw : m, n \in \mathbb{Z}, c \in \{0, 1\}\},$$

with

$$t_1 := \begin{pmatrix} \sqrt{3} \\ 0 \end{pmatrix}, \quad t_2 := \begin{pmatrix} \sqrt{3}/2 \\ 3/2 \end{pmatrix}, \quad \text{and} \quad w := \begin{pmatrix} 0 \\ 1 \end{pmatrix}.$$

Note that the minimal distance between points in \mathcal{L} is 1.

We denote a *configuration* of n atoms by $C_n := \{x_1, \dots, x_n\} \in \mathbb{R}^{2n}$, the distance between two atoms, x_i and x_j , by ℓ_{ij} , and the counterclockwise-oriented angle

6 *Elisa Davoli, Paolo Piovano, and Ulisse Stefanelli*

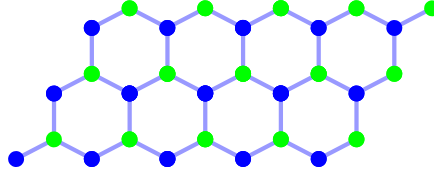


Fig. 1. An example of a subset of \mathcal{L} .

between the two segments $x_i - x_j$ and $x_k - x_j$ by θ_{ijk} . The *energy* of a configuration C_n is defined as

$$E(C_n) := E_2(C_n) + E_3(C_n) = \frac{1}{2} \sum_{i \neq j} v_2(\ell_{ij}) + \sum_{(i,j,k) \in \mathcal{A}} v_3(\theta_{ijk}) \quad (2.1)$$

where $v_2 : [0, \infty) \rightarrow [-1, \infty]$ and $v_3 : [0, 2\pi] \rightarrow [0, \infty)$ are the two-body and the three-body interaction potentials. We notice that the energy is invariant under rotations and translations. Two atoms x_i and x_j are said to be *bonded*, or there is an (*active*) *bond* between x_i and x_j , if $1 \leq \ell_{ij} < \sqrt{2}$. The index set \mathcal{A} in (2.1) is defined as the set of all triples (i, j, k) for which the angle θ_{ijk} separates two active bonds. We will always assume that $v_2(1) = -1$ and that $v_2(\ell)$ vanishes for $\ell \geq \sqrt{2}$ (see below). We work under the assumption that v_3 reaches its minimum value only at the angles $\pi/3$ and $2\pi/3$, and that ground states are subsets of the hexagonal lattice. We use the standard notation for the right- and left-continuous integer-parts: $\lfloor x \rfloor := \max\{z \in \mathbb{Z} : z \leq x\}$ and $\lceil x \rceil := \min\{z \in \mathbb{Z} : x \leq z\}$, respectively.

Under suitable assumptions on the potentials v_2 and v_3 , it was established in Ref. 32 that all ground-state configurations are (isometric to) subsets of the hexagonal lattice \mathcal{L} and that the value of the energy for every ground state with n atoms is given by

$$e_n := -\left\lfloor \frac{3n}{2} - \sqrt{\frac{3n}{2}} \right\rfloor. \quad (2.2)$$

From this point on all configurations are hence seen as subsets of \mathcal{L} .

The *bond graph* of a configuration C_n is the graph consisting of all its vertices and active bonds. For every atom $x_i \in C_n$, we indicate by $b(x_i)$ the number of active bonds of C_n with an endpoint in x_i . Denoting by $B(C_n)$ the total number of bonds in C_n , there holds

$$B(C_n) = \frac{1}{2} \sum_{i=1}^n b(x_i).$$

A configuration C_n is said to be *connected* if for every two atoms $y_1, y_2 \in C_n$ there exists a collection of atoms $x_1, \dots, x_i \in C_n$ such that y_1 is bonded to x_1 , x_i is bonded to y_2 , and every atom x_j , with $2 \leq j \leq i-1$ is bonded both to x_{j-1} and to

x_{j+1} . We call *minimal simple cycles* of a configuration all the simple cycles in the graph that are hexagons of side 1.

The *area* $A(C_n)$ of a configuration C_n is given by the number of minimal simple cycles of C_n . Denoting by $F(C_n) \subset \mathbb{R}^2$ the closure of the union of the regions enclosed by the minimal simple cycles of C_n , and by $G(C_n) \subset \mathbb{R}^2$ the union of all bonds which are not included in $F(C_n)$, the *perimeter* P of a configuration C_n is defined as

$$P(C_n) := \mathcal{H}^1(\partial F(C_n)) + 2\mathcal{H}^1(G(C_n)),$$

where \mathcal{H}^1 is the one-dimensional Hausdorff measure. As already observed in Ref. 30, there holds

$$P(C_n) = \lim_{\varepsilon \searrow 0} \mathcal{H}^1\left(\partial(\partial F(C_n) \cup G(C_n) + B_\varepsilon)\right)$$

where $B_\varepsilon = \{y \in \mathbb{R}^2 \mid |y| \leq \varepsilon\}$.

With a slight abuse of notation, the symbol $|\cdot|$ will denote, according to the context, both the absolute value of a real number and the cardinality of a set.

We will often use the notion of *edge boundary* Θ of a configuration with respect to a reference lattice: this is the union of unit segments in the reference lattice that are not included in the graph of C_n but share one and only one endpoint with C_n ,

$$\Theta(C_n) := \{(x, y) \in (\mathcal{L})^2 : x \in C_n, y \notin C_n\}.$$

The *edge perimeter* of a configuration C_n will be defined as the number of segments belonging to its edge boundary.

For every configuration $C_n := \{x_1, \dots, x_n\}$ in \mathcal{L} , we denote by μ_{C_n} the *empirical measure associated to the rescaled configuration* $\{x_1/\sqrt{n}, \dots, x_n/\sqrt{n}\}$, that is,

$$\mu_{C_n} := \frac{1}{n} \sum_i \delta_{x_i/\sqrt{n}}. \quad (2.3)$$

Given a Lebesgue measurable set $A \subset \mathbb{R}^2$, we will designate by $\mathcal{L}^2(A)$ its two-dimensional Lebesgue measure. For any bounded Radon measure μ , the symbol $\|\mu\|$ will represent its total variation in \mathbb{R}^2 , whereas $\|\mu\|_F$ will be the *flat norm* of μ , defined as

$$\|\mu\|_F := \sup \left\{ \int_{\mathbb{R}^2} \varphi d\mu : \varphi \text{ is Lipschitz with } \|\varphi\|_{W^{1,\infty}(\mathbb{R}^2)} \leq 1 \right\}. \quad (2.4)$$

The set of bounded Radon measures on \mathbb{R}^2 will be denoted by $M_b(\mathbb{R}^2)$.

8 *Elisa Davoli, Paolo Piovano, and Ulisse Stefanelli*

3. Discrete isoperimetric inequality

In this section we prove that connected configurations satisfy a discrete isoperimetric inequality, and we characterize ground states as configurations realizing the isoperimetric equality. We first deduce some preliminary relations between the area, the perimeter, the edge perimeter, and the energy of configurations. Let C_n be a configuration. Then

$$E(C_n) = -B(C_n) = -\frac{1}{2} \sum_{i=1}^n b(x_i).$$

Since every atom in \mathcal{L} has exactly 3 bonds, we have

$$|\Theta(C_n)| = \sum_{i=1}^n (3 - b(x_i)), \quad (3.1)$$

and the energy and the edge perimeter of configurations are related by

$$E(C_n) = -\frac{3}{2}n + \frac{1}{2}|\Theta(C_n)|. \quad (3.2)$$

Recalling that every minimal simple cycle of C_n consists of 6 bonds, we have

$$\begin{aligned} 6A(C_n) &= 2B(C_n \cap F(C_n)) - B(C_n \cap \partial F(C_n)) \\ &= -2E(C_n \cap F(C_n)) - \mathcal{H}^1(\partial F(C_n)). \end{aligned}$$

On the other hand,

$$\mathcal{H}^1(G(C_n)) = B(C_n \cap G(C_n)) = -E(C_n \cap G(C_n)).$$

Hence, we obtain

$$\begin{aligned} P(C_n) &= \mathcal{H}^1(\partial F(C_n)) + 2\mathcal{H}^1(G(C_n)) \\ &= -2E(C_n \cap F(C_n)) - 6A(C_n) - 2E(C_n \cap G(C_n)) \\ &= -2E(C_n) - 6A(C_n), \end{aligned}$$

that is

$$E(C_n) = -3A(C_n) - \frac{1}{2}P(C_n). \quad (3.3)$$

In conclusion, we can express the energy of a hexagonal configuration C_n as a linear combination of its area and its perimeter. Likewise, in view of (3.2), the edge perimeter satisfies

$$|\Theta(C_n)| = 3n - 6A(C_n) - P(C_n).$$

The following result is a direct corollary of Theorem 7.3 (page 142) in Ref. 23.

Proposition 3.1. *There exists a total order $\tau : \mathbb{N} \rightarrow \mathcal{L}$ such that for all $n \in \mathbb{N}$ the configuration D_n defined by $D_n := \{x_{\tau(1)}, \dots, x_{\tau(n)}\}$ (which we call daisy) minimizes E over all configurations with n atoms, i.e.*

$$E(D_n) = \min_{C_n \in \mathcal{L}} E(C_n) = e_n, \quad (3.4)$$

where e_n is the quantity defined in (2.2).

The total order in Proposition 3.1 is nonunique. For the sake of definiteness we fix here our attention on a specific order τ , as described in Ref. 32. For $n = 6k^2$, $k \in \mathbb{N}$, the sequence $\{D_{6k^2}\}$ is defined inductively as follows: D_6 is a minimal simple cycle in \mathcal{L} , and D_{24} is obtained by externally attaching to all bonds of D_6 another hexagon. D_{6k^2} is then defined recursively.

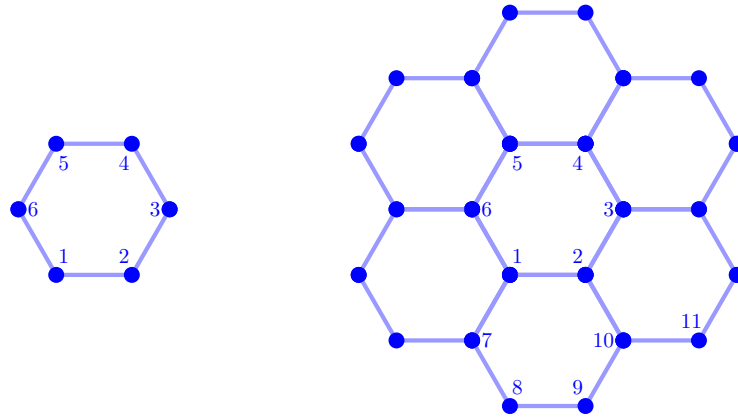


Fig. 2. The daisies D_6 and D_{24} and the total order τ .

For $k, m \in \mathbb{N}$, and $0 < m < 12k(k+1)$, D_{6k^2+m} is constructed as in the proof of Proposition 5.1 (Step 1) in Ref. 32. In view of Proposition 3.1, it is always possible to add one atom to a daisy D_n so that the new configuration with $n+1$ points is still a ground state.

To every configuration $C_n \subset \mathcal{L}$, we associate a weight function

$$\Delta_{C_n} : C_n \rightarrow \{0, 1, 2\},$$

defined as

$$\Delta_{C_n}(x) := |\{y \in C_n : (x, y) \in C_n \times C_n, y <_\tau x\}|,$$

for every $x \in C_n$, and we rewrite C_n as the union

$$C_n = \bigcup_{k=0}^2 C_n^k$$

where

$$C_n^k := \{x \in C_n : \Delta_{C_n}(x) = k\}$$

10 *Elisa Davoli, Paolo Piovano, and Ulisse Stefanelli*

for $k = 0, \dots, 2$. In particular, $|C_n^0|$ corresponds to the number of *connected components* of C_n .

The next proposition allows us to express the energy, the perimeter, the edge perimeter, and the area of a configuration C_n as a function of the cardinality of the sets C_n^k .

Proposition 3.2. *Let C_n be a configuration in \mathcal{L} . Then,*

$$E(C_n) = -|C_n^1| - 2|C_n^2|, \quad (3.5)$$

$$A(C_n) = |C_n^2|, \quad (3.6)$$

$$P(C_n) = 2|C_n^1| - 2|C_n^2|, \quad (3.7)$$

$$|\Theta(C_n)| = 3|C_n^0| + |C_n^1| - |C_n^2|, \quad (3.8)$$

for every $n > 1$. Moreover,

$$E(C_n) = -3A(C_n) - |\Theta(C_n)| + 3|C_n^0|. \quad (3.9)$$

Proof. We first observe that

$$E(C_n) = -\sum_{i=1}^n \Delta_{C_n}(x_i).$$

For $i = 0, \dots, n-1$, let C_i be the subset of C_n containing its first i points according to the total order τ . If $x_{\tau(i)} \in C_n^0$, then

$$A(C_i) - A(C_{i-1}) = 0, \quad P(C_i) - P(C_{i-1}) = 0, \quad |\Theta(C_i)| - |\Theta(C_{i-1})| = 3; \quad (3.10)$$

if $x_{\tau(i)} \in C_n^1$, then

$$A(C_i) - A(C_{i-1}) = 0, \quad P(C_i) - P(C_{i-1}) = 2, \quad |\Theta(C_i)| - |\Theta(C_{i-1})| = 1; \quad (3.11)$$

whereas, if $x_{\tau(i)} \in C_n^2$, we have

$$A(C_i) - A(C_{i-1}) = 1, \quad P(C_i) - P(C_{i-1}) = -2, \quad |\Theta(C_i)| - |\Theta(C_{i-1})| = -1. \quad (3.12)$$

Properties (3.5)–(3.8) follow from (3.10)–(3.12). Claim (3.9) is a direct consequence of (3.3), (3.7), and (3.8). \square

In view of Proposition 3.2 we obtain the following.

Proposition 3.3. *The following assertions are equivalent and hold true for every connected hexagonal configuration C_n :*

- (i) $|\Theta(D_n)| \leq |\Theta(C_n)|$;
- (ii) $P(D_n) \leq P(C_n)$;
- (iii) $A(D_n) \geq A(C_n)$.

Proof. The first assertion is a direct consequence of (3.2) and (3.4), and is equivalent to (ii) by (3.7) and (3.8). The equivalence between (ii) and (iii) follows by (3.3) and (3.4). \square

We are now in a position to characterize connected ground states as extremizers of a discrete isoperimetric problem.

Proposition 3.4. *Every connected configuration C_n satisfies*

$$\sqrt{A(C_n)} \leq k_n P(C_n), \quad (3.13)$$

where

$$k_n := \frac{\sqrt{[(\alpha_n)^2 - \alpha_n] - n + 1}}{4(\alpha_n)^2 - 4[(\alpha_n)^2 - \alpha_n] - 6}, \quad (3.14)$$

and $\alpha_n := \sqrt{3n/2}$.

Moreover, connected ground states correspond to those configurations for which (3.13) holds with equality, and, equivalently, to those configurations that attain the maximum area

$$a_n := -n + [(\alpha_n)^2 - \alpha_n] + 1,$$

and the minimum perimeter

$$p_n := 4(\alpha_n)^2 - 4[(\alpha_n)^2 - \alpha_n] - 6.$$

Proof. We claim that

$$\sqrt{A(D_n)} = k_n P(D_n). \quad (3.15)$$

In fact, in view of (3.5) and Theorem 3.1, there holds

$$e_n = E(D_n) = -|D_n^1| - 2|D_n^2|,$$

whereas by (3.2) and (3.8),

$$3n + 2e_n = |\Theta(D_n)| = 3 + |D_n^1| - |D_n^2|,$$

where e_n is the ground state energy defined in (2.2). Solving the previous system of equations we deduce

$$|D_n^1| = 2n + e_n - 2, \quad (3.16)$$

and

$$|D_n^2| = -n - e_n + 1. \quad (3.17)$$

Claim (3.15) follows from (3.6), (3.7), (3.16), and (3.17), by observing that

$$\sqrt{A(D_n)} = \sqrt{|D_n^2|} = \sqrt{-n - e_n + 1}$$

12 *Elisa Davoli, Paolo Piovano, and Ulisse Stefanelli*

$$= k_n(6n + 4e_n - 6) = k_n(2|D_n^1| - 2|D_n^2|) = k_n P(D_n).$$

Inequality (3.13) is a direct consequence of (3.15) and Proposition 3.3. By Proposition 3.3 and (3.2), connected ground states G_n satisfy

$$|\Theta(G_n)| = e_n + \frac{3}{2}n$$

and attain the maximum area and the minimum perimeter. The values of a_n and p_n follow from (3.8), (3.7), and (3.9). \square

4. Equilibrium shapes of graphene samples

In this section we characterize the edge geometry of graphene samples. We first introduce a few definitions.

Definition 4.1. For every $s \in \mathbb{N}$ we define the set \mathcal{H}_s^Z of *zigzag hexagons of side s* as

$$\mathcal{H}_s^Z := \{D_{6s^2} + q : q \in \mathcal{L}\}$$

(for all $s \in \mathbb{N}$, the configuration D_{6s^2} is a complete *hexagon* of hexagons). For $s \in \mathbb{N}$, $s \geq 3$, the set \mathcal{H}_s^A of *armchair hexagons of side s* is defined as

$$\mathcal{H}_s^A := \{A_s + q : q \in \mathcal{L}\}.$$

In the expression above, A_3 is given by the union of D_{24} with 6 extra minimal simple cycles, glued externally to the center of each side of D_{24} (see Figure 3). For $s > 3$, A_s is defined recursively by adding an extra armchair layer of minimal simple cycles to A_{s-1} . We point out that the construction is different for s even and s odd (see Figure 3).

4.1. Proof of Theorem 1.1

The optimality of zigzag hexagons follows in view of Definition 4.1 and Proposition 3.1.

We claim that for every $s \in \mathbb{N}$, $s \geq 3$, there holds

$$P(A_s) > p_{|A_s|}. \tag{4.1}$$

Indeed, by the definition of A_s we have $|A_3| = 42$, and for $s > 3$

$$|A_s| = |A_{s-1}| + \begin{cases} 6(2s-1) & \text{if } s \text{ is even,} \\ 6s & \text{if } s \text{ is odd,} \end{cases}$$

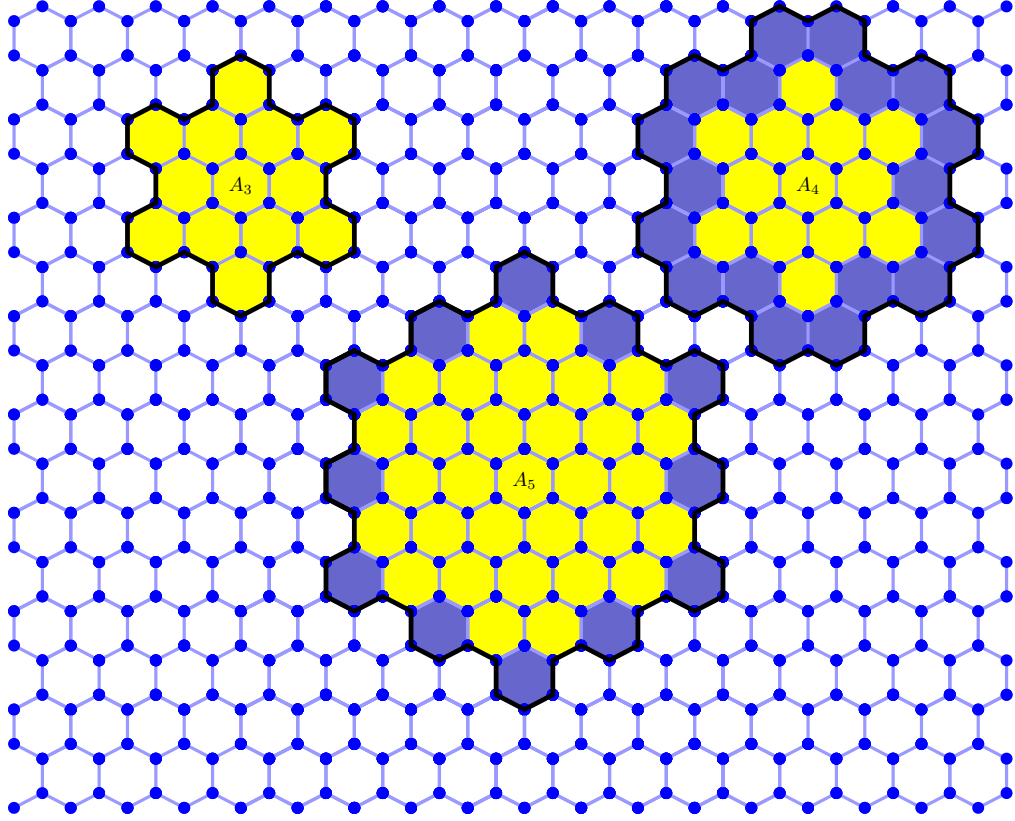


Fig. 3. The armchair hexagons A_3 , A_4 and A_5 . Each armchair hexagon A_s for $s > 3$ is obtained by adding a layer of extra minimal simple cycles (in blue) to the corresponding armchair hexagon A_{s-1} (in yellow). Notice the different structure for s even and for s odd.

that is

$$|A_s| = \frac{9}{2}s^2 + \begin{cases} 3s & \text{if } s \text{ is even,} \\ \frac{3}{2} & \text{if } s \text{ is odd.} \end{cases}$$

On the other hand, the perimeter of each armchair hexagon A_s is given by

$$P(A_s) = 12s - 6. \quad (4.2)$$

For s odd, we have

$$\alpha_{|A_s|} = \sqrt{\frac{3|A_s|}{2}} = \frac{3}{2}s\sqrt{3 + \frac{1}{s^2}}.$$

Hence,

$$\alpha_{|A_s|}^2 = \frac{9}{4}(3s^2 + 1) \in \mathbb{N},$$

14 *Elisa Davoli, Paolo Piovano, and Ulisse Stefanelli*

and

$$\alpha_{|A_s|}^2 - [\alpha_{|A_s|}^2 - \alpha_{|A_s|}] = \left\lceil \frac{3}{2}s\sqrt{3 + \frac{1}{s^2}} \right\rceil.$$

In view of Proposition 3.4 there holds

$$\begin{aligned} p_{|A_s|} &= 4\alpha_{|A_s|}^2 - 4[\alpha_{|A_s|}^2 - \alpha_{|A_s|}] - 6 \\ &\leq 4\left(\frac{3}{2}s\sqrt{3 + \frac{1}{s^2}}\right) - 2 \\ &= 6\sqrt{3}s + \frac{6}{s\left(\sqrt{3} + \sqrt{3 + \frac{1}{s^2}}\right)} - 2 \\ &< 6\sqrt{3}s + \frac{\sqrt{3}}{s} - 2 < 12s - 6 \end{aligned} \tag{4.3}$$

for $s \geq 3$.

By combining (4.2) and (4.3) we obtain claim (4.1) for s odd. The result for s even, $s \geq 4$ follows via analogous computations. In view of Proposition 3.4 and (4.1) armchair hexagons are not extremizers of the isoperimetric inequality, and hence are not ground states. \square

5. The radius of the n -Wulff shape

For simplicity in what follows we will refer to the elements of \mathcal{H}_s^Z as *hexagons of side s* , omitting the word *zigzag*. We first introduce the notion of *maximal hexagon* associated to a ground state.

Let G_n be a ground state in the hexagonal lattice \mathcal{L} . Let

$$r_{G_n} := \max \left\{ s \in \mathbb{N} : \text{there exists a point } q \in \mathcal{L} \text{ such that } D_{6s^2} + q \subseteq G_n \right\}.$$

For every $q \in \mathcal{L}$ such that $D_{6r_{G_n}^2} + q \subset G_n$, we will refer to the set

$$H_{G_n} := D_{6r_{G_n}^2} + q,$$

as a *maximal hexagon associated to G_n* . We recall that

$$G_n = \bigcup_{k=0}^2 G_n^k,$$

where

$$G_n^k := \{x \in G_n : \Delta_{G_n}(x) = k\}.$$

Let us preliminary check that maximal hexagons are non-degenerate for $n > 6$. We recall that the n -Wulff shape W_n is the zigzag hexagon centered in the origin with side r_n (see (1.6)), i.e.,

$$W_n := D_{6r_n^2}.$$

Proposition 5.1. *The radius r_n of the n -Wulff shape W_n (see (1.6) and Theorem 1.2) with $n > 6$, satisfies $r_n \geq 1$.*

Proof.

Let $n \in \mathbb{N}$ be such that there exists a ground state G_n with $r_{G_n} = 0$. Then G_n does not contain any set of the form $D_6 + q$ with $q \in \mathcal{L}$, that is, for every $x \in G_n$, there holds (see (3.12))

$$x \notin G_n^2. \quad (5.1)$$

By (3.11) and (3.12), property (5.1) is equivalent to the claim that every element of $G_n \setminus G_n^0$ contributes to the overall perimeter of G_n , and the contribution of each element is exactly 2. Since we are assuming that G_n is connected (i.e. $|G_n^0| = 1$), this implies that

$$P(G_n) \geq 2(n-1).$$

By Proposition 3.4 it follows that

$$4(\alpha_n)^2 - 4[(\alpha_n)^2 - \alpha_n] - 6 = P(D_n) = p_n \geq 2(n-1),$$

which in turn implies

$$n-1 \geq [(\alpha_n)^2 - \alpha_n] \geq (\alpha_n)^2 - \alpha_n,$$

and finally yields $n - \sqrt{6n} \leq 0$, that is $0 \leq n \leq 6$. \square

Fix $n \in \mathbb{N}$ and let G_n be a connected ground state. We aim at proving an estimate from below on the radius r_{G_n} of H_{G_n} in terms of the number n of atoms. We first introduce some definitions.

Definition 5.1 (zigzag path). Let ℓ be a line orthogonal to one of the three diameters of a minimal simple cycle of the lattice and intersecting \mathcal{L} . The *zigzag path* identified by ℓ is the union of points $p \in \mathcal{L}$ such that either $p \in \ell$ or there exists a minimal simple cycle H of \mathcal{L} such that p belongs to H , and the two atoms in H bonded to P are in ℓ . Note that each point of a zigzag path divides it into two *half zigzag paths* (see Figure 5).

Let $P_1, \dots, P_4 \in \mathcal{L} \cap \partial F(C_n)$ be such that P_1 is bonded to P_2 , and for $i = 2, 3$ the point P_i is bonded both to P_{i-1} and P_{i+1} . If there exists a unique zigzag path passing through all the points P_1, \dots, P_4 we will say that this zigzag path is a *side* of C_n . If two different (non parallel) zigzag path intersect in the unitary segment joining P_2 and P_3 we will refer to this segment as a *corner edge* of C_n (see Figure 4).

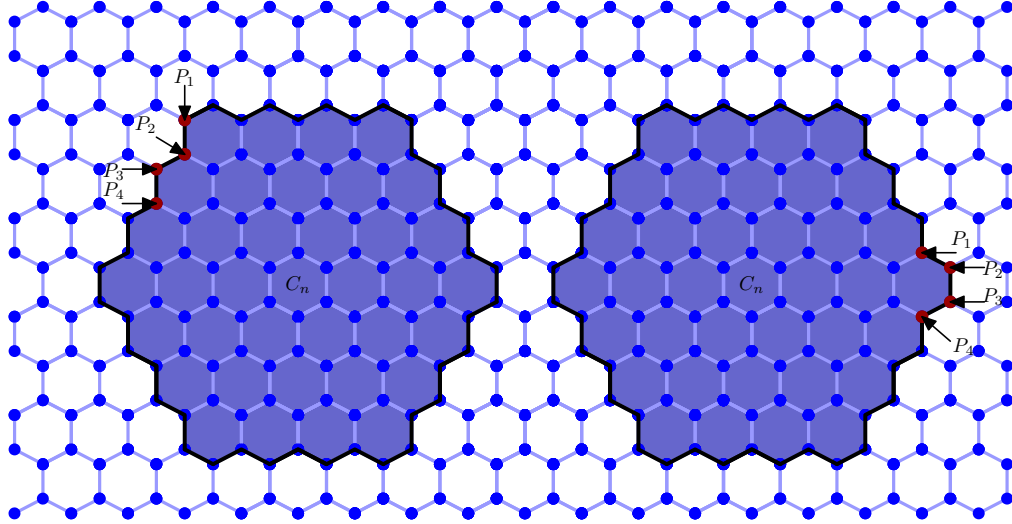


Fig. 4. On the left, the points P_1, \dots, P_4 belong to a *side* of C_n , on the right the segment joining P_2 and P_3 is a *corner edge* of C_n .

We will say that C_n has an *angle* α in a corner edge v (or in a point P) if the two lines ℓ_α^1 and ℓ_α^2 , identifying the sides of C_n and passing through v (respectively, P), intersect forming an angle of width α . The choice of α or $2\pi - \alpha$ will be clear from the context. Alternatively, we will say that the zigzag paths associated to ℓ_α^1 and ℓ_α^2 form an angle α with (or in) v (respectively, P).

Finally, if $S \subset \mathcal{L}$ is such that $\partial(F(S)) \cap \mathcal{L}$ (see Section 2) is the union of two zigzag paths forming an angle α , we will call S an *angular sector of width* α , see Figure 5.

By Proposition 5.1 we can assume that $r_{G_n} \geq 1$. Let v_0, \dots, v_5 be the corner edges of H_{G_n} , where v_0 is assumed to be lying on the x -axis (without loss of generality), and v_1, \dots, v_5 are numbered counterclockwise starting from v_0 . For $k = 0, \dots, 4$, let s_k be the zigzag path joining v_k and v_{k+1} , and let s_5 be the zigzag path joining v_5 and v_0 . Let l_k be the line identifying the path s_k , and denote by ν_k the unit normal to l_k pointing toward the exterior of H_{G_n} . We define

$$\lambda_k := \max\{j \in \mathbb{N} : s_k^j \cap G_n \neq \emptyset\}, \quad (5.2)$$

where

$$s_k^j := s_k + j\nu_k$$

for $j \in \mathbb{N}$. Let also π_k be the subset of \mathcal{L} such that $\partial F(\pi_k) = s_k$ and $\mathring{F}(\pi_k) \cap H_{G_n} = \emptyset$.

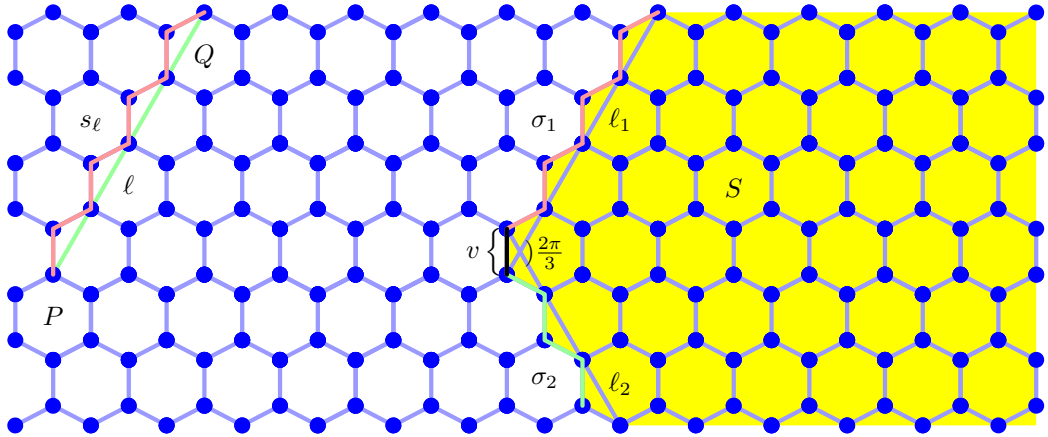


Fig. 5. On the left, the zigzag path s_ℓ originated by the line ℓ . On the right, the two zigzag paths σ_1 and σ_2 intersect in the corner edge v , forming an angle $2\pi/3$. The associated angular sector S is marked in yellow.

We show now that ground states satisfy a connectedness property with respect to zigzag paths.

Definition 5.2 (hex-connectedness). Let \mathcal{S} be a subset of \mathcal{L} and let $P \in \mathcal{L}$. We say that P disconnects a zigzag path in \mathcal{S} if $P \notin \mathcal{S}$ and there exist $P_a, P_b \in \mathcal{S}$ such that P_a and P_b are joined by a zigzag path passing through P .

Let \mathcal{S} be a subset of \mathcal{L} . We say that \mathcal{S} is *hex-connected* if every $P \in \mathcal{L}$ disconnects at most one zigzag path in \mathcal{S} .

Notice that from every point $P \in \mathcal{L}$ there are exactly three nonparallel lines which depart from P and identify a zigzag path (see Definition 5.1).

Proposition 5.2. *Ground states are hex-connected.*

Proof. For the sake of contradiction assume that there exists a ground state G_n which is not hex-connected. Then there exists a point $P \in \mathcal{L}$ which disconnects two zigzag paths in G_n . In particular, there exists a line ℓ_0 orthogonal to one of the diameters of a minimal simple cycle of the lattice, and intersecting \mathcal{L} , such that the two half zigzag paths starting from P and identified by ℓ_0 are both intersecting G_n . Let ℓ_1, \dots, ℓ_m be the lines parallel to ℓ_0 , intersecting G_n , and such that for every $i = 1, \dots, m$, the distance between ℓ_i and ℓ_0 is given by $3n_i/2$, where $n_i \in \mathbb{N}$. For $i = 0, \dots, m$, let c_i be the number of points of G_n contained in the zigzag path identified by ℓ_i .

We first rearrange the set $\{c_i\}$ in a decreasing order, constructing another set

18 *Elisa Davoli, Paolo Piovano, and Ulisse Stefanelli*

$\{d_i\}$ with the property that $d_0 \geq d_1 \geq \dots \geq d_m$. Then, we separate the elements of $\{d_i\}$ having odd indexes from those having even indexes and we consider a new family $\{f_i\}$ obtained by first taking into account the elements of $\{d_i\}$ with even indexes, in decreasing order with respect to their indexes, and then the elements of $\{d_i\}$ having odd indexes, with increasing order with respect to their indexes. In particular we define

$$f_i := \begin{cases} d_{m-2i} & i = 0, \dots, \frac{m}{2} \\ d_{2i-m-1} & i = \frac{m}{2} + 1, \dots, m \end{cases} \quad \text{if } m \text{ is even, and}$$

$$f_i := \begin{cases} d_{m-1-2i} & i = 0, \dots, \frac{(m-1)}{2} \\ d_{2i-m} & i = \frac{(m+1)}{2}, \dots, m \end{cases} \quad \text{if } m \text{ is odd.}$$

The set $\{f_i\}$ constructed above has the property that its central elements have the maximum value, and the values of the elements decrease in an alternated way by moving from the center of $\{f_i\}$ toward $i = 0$ and $i = m$. Let \bar{i} and $\bar{i} + 1$ be the indexes corresponding to the two central elements of the set $\{f_i\}$, if m is odd, and to the central element of $\{f_i\}$ and the maximum between its two neighbors, if m is even. As an example, if we start with a set $\{c_i\} = \{3, 4, 7, 8, 2, 2, 8\}$, the family $\{d_i\}$ is given by $\{8, 8, 7, 4, 3, 2, 2\}$ and the set $\{f_i\}$ by $\{2, 3, 7, 8, 8, 4, 2\}$. Here $\bar{i} = 4$.

Fix two points $P_i, P_{i+1} \in \mathcal{L}_h$ such that the segment $P_i P_{i+1}$ has length one and is orthogonal to ℓ_0 . Let σ_1 and σ_2 be two half-zigzag paths, starting from P_i and P_{i+1} , respectively, forming an angle $2\pi/3$ with $P_i P_{i+1}$, and such that there exists a convex region S of the plane whose boundary is given by σ_1 , σ_2 , and $P_i P_{i+1}$.

Consider the points $P_0, \dots, P_{\bar{i}-1} \in \sigma_1$, defined as

$$|P_i - P_j| = (\bar{i} - j)\sqrt{3}, \quad j = 0, \dots, \bar{i} - 1.$$

Analogously, consider the points $P_{\bar{i}+2}, \dots, P_m \in \sigma_2$, satisfying

$$|P_{i+1} - P_j| = (j - \bar{i})\sqrt{3}, \quad j = \bar{i} + 2, \dots, m.$$

For $j = 0, \dots, m$, let $\tilde{\ell}_j$ be the line parallel to ℓ_0 and passing through P_j . To construct the set \tilde{G}_n we consider f_j consecutive points in S on the zigzag path identified by each line $\tilde{\ell}_j$, starting from P_j (see figure 5). The set \tilde{G}_n is clearly hex-connected, the number of bonds in the zigzag paths identified by the lines parallel to ℓ_0 has increased, and the number of bonds between parallel zigzag paths has not decreased. Hence

$$E(\tilde{G}_n) < E(G_n),$$

providing a contradiction to the optimality of the ground state G_n . \square

As a corollary of Proposition 5.2 it follows that ground states have no *vacancies*.

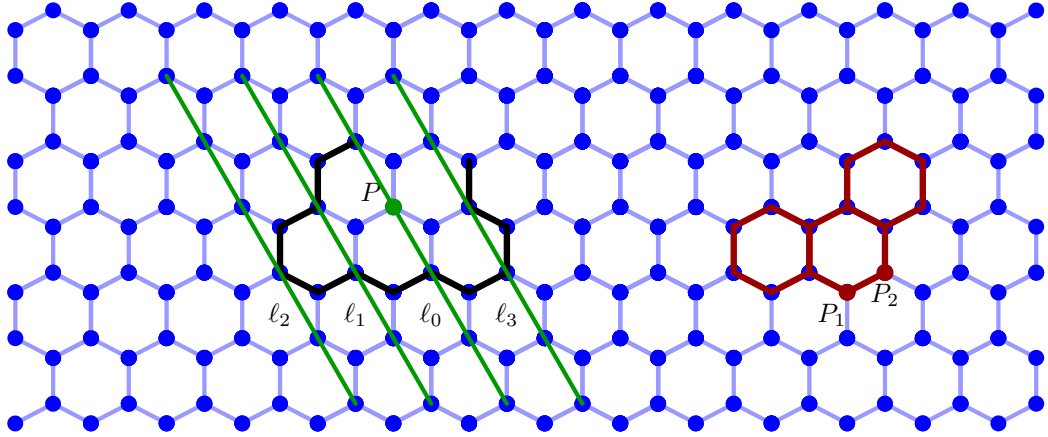


Fig. 6. A configuration C_n before (in black) and after (in red) the rearrangement described in Proposition 5.2

Proposition 5.3. *Let G_n be a ground state. Then $F(G_n)$ is simply connected.*

Proof. By contradiction, if $F(G_n)$ is not simply connected then there exists a point in \mathcal{L} that disconnects three zigzag paths in G_n . Therefore G_n is not hex-connected \square

We conclude this overview on connectedness properties of ground states with the following proposition.

Proposition 5.4. *Ground states are connected.*

We omit the proof of this result as it follows by adapting the proof of Proposition 5.2.

In view of Propositions 5.2–5.4, the quantity λ_k defined in (5.2) provides the number of nonempty parallel zigzag paths of atoms in $G_n \cap \pi_k$. By the definition of τ , each partially full level of atoms around H_{G_n} is characterized by the fact that the difference between the number of points on the level having weight one and those having weight two is strictly positive. To be precise,

$$\sum_{k=0}^5 \lambda_k \leq |G_n^1 \setminus H_{G_n}| - |G_n^2 \setminus H_{G_n}|.$$

On the other hand, by (3.11) and (3.12),

$$|G_n^1 \setminus H_{G_n}| - |G_n^2 \setminus H_{G_n}| = \frac{P(G_n) - P(H_{G_n})}{2} = \frac{p_n}{2} - 6r_{G_n} + 3,$$

20 *Elisa Davoli, Paolo Piovano, and Ulisse Stefanelli*

thus yielding

$$\sum_{k=0}^5 \lambda_k \leq \frac{p_n}{2} - 6r_{G_n} + 3. \quad (5.3)$$

Given a ground state G_n and its maximal hexagon $H_{G_n} := D_{6r_{G_n}^2} + q$, denote by $H_{G_n}^+$ and $H_{G_n}^{++}$ the sets $H_{G_n}^+ := D_{6(r_{G_n}+1)^2} + q$, and $H_{G_n}^{++} := D_{6(r_{G_n}+2)^2} + q$, respectively. Denote by v'_i and v''_i , $i = 0, \dots, 5$, the corner edges of $H_{G_n}^+$ and $H_{G_n}^{++}$, respectively, with the convention that both v'_i and v''_i are parallel to v_i . For $i = 0, \dots, 5$, let V_i^1 and V_i^2 be the two extrema of v_i , numbered counterclockwise. Let $(V_i^1)^1$, $(V_i^1)^2$, $(V_i^2)^1$, $(V_i^2)^2$, s'_i , and s''_i be defined accordingly.

In the remaining part of this subsection we provide a characterization of the geometry of $G_n \setminus H_{G_n}^+$, by subdividing this set into *good* polygons P_k and *bad* polygons T_k , and by showing that the cardinality of $G_n \setminus H_{G_n}^+$ is, roughly speaking, the same as the one of the union of *good* polygons.

We first prove that, by the optimality of H_{G_n} , there exists a corner edge of $H_{G_n}^{++}$ which does not intersect G_n .

Proposition 5.5. *Let G_n be a ground state, and H_{G_n} be its maximal hexagon. Then there exists a corner edge v''_j of $H_{G_n}^{++}$, $j = 0, \dots, 5$, which does not intersect G_n .*

Proof. By the maximality of H_{G_n} , there exists a point $P \in \partial F(H_{G_n}^+)$ such that $P \notin G_n$.

If P does not disconnect s'_i then either v'_i or v'_{i+1} do not intersect G_n . By the hex-connectedness of G_n (see Proposition 5.2) then also the corresponding corner edge of $H_{G_n}^{++}$ does not intersect G_n , and we obtain the thesis.

Assume now that P disconnects s'_i . Since G_n is hex-connected, the point P does not disconnect any other zigzag path. Therefore there exists an angular sector S centered in P and of width $\pi/3$ such that

$$S \cap G_n = \emptyset. \quad (5.4)$$

Assume by contradiction that all corner edges of $H_{G_n}^{++}$ intersect G_n . In view of (5.4), the set $(G_n \setminus H_{G_n}) \cap \pi_i$ is subdivided into two components. Denoting them by Γ_1 and Γ_2 , we have that $\Gamma_j \cap s_i^1 \neq \emptyset$ and $\Gamma_j \cap s_i^2 \neq \emptyset$, for $j = 1, 2$. Without loss of generality we can assume that $\Gamma_1 \cap s_i^{\lambda_i} \neq \emptyset$. Consider now the set $M := \Gamma_1 \cap (s_i^{\lambda_i} \cup s_i^{\lambda_i-1})$. We claim that we can construct a new set \tilde{G}_n , by rearranging the atoms of M and by leaving the other elements of G_n fixed, such that

$$E(\tilde{G}_n) < E(G_n). \quad (5.5)$$

There are three possible scenarios.

Case 1: Γ_1 contains at least two points P_a and P_b with the property that for each of them there is no minimal cycle passing through it and entirely contained in G_n . We proceed by moving the two points to $s_i^1 \cap (\mathcal{L} \setminus G_n)$ in such a way that P_a is bonded to Γ_2 . If possible, we move also P_b to $s_i^1 \cap (\mathcal{L} \setminus G_n)$ so that P_a and P_b are bonded. If this is not possible because $s_i \cap (\mathcal{L} \setminus G_n)$ contains only one element, then we already created an extra bond. With this procedure we loose two bonds when removing P_a and P_b from Γ_1 , but we gain at least three bonds when we attach them to Γ_2 , therefore the total energy strictly decreases.

Case 2: in Γ_1 there exists exactly one point P_a with the property that there is no minimal cycle containing it and entirely contained in G_n . We argue moving this single point to $s_i^1 \cap (\mathcal{L} \setminus G_n)$ in such a way that P_a is bonded to Γ_2 . Afterward, we move iteratively all the (remaining) points in $s_i^{\lambda_i} \cap \Gamma_1$ to $s_i^1 \cap (\mathcal{L} \setminus G_n)$ (in the same way as described in Case 1 for P_b). If after moving P_a there are no remaining points in $s_i^{\lambda_i} \cap \Gamma_1$, we apply the same rearrangement to $s_i^{\lambda_i - 1} \cap \Gamma_1$ (note that $\lambda_i \geq 2$ because all corner edges of $H_{G_n}^{++}$ intersect G_n). As a result of the procedure described above, the energy is strictly decreased. If at any moment during the process of attaching points to Γ_2 we create a bond between Γ_1 and Γ_2 , we stop the rearrangement as the number of bonds has strictly increased.

Case 3: every point of Γ_1 belongs to a minimal cycle entirely contained in G_n . In this case we first move all points in $s_i^{\lambda_i} \cap \Gamma_1$ but one, in the same way as described in Cases 1 and 2. As a result of this procedure, either we already created an extra bond (and hence there is nothing left to prove) or we are now in the same situation described in Case 2. The thesis follows then arguing exactly as in Case 2. \square

We proceed by showing that for every hexagon of side $r_{G_n} + 2$ there exists an angular sector of width $\pi/3$, and centered in one of its corner edges, which does not intersect G_n .

Proposition 5.6. *Let G_n be a ground state, and H_{G_n} be its maximal hexagon. Then*

- (i) *There exists a corner edge v_i'' of $H_{G_n}^{++}$, $i = 0, \dots, 5$, and an angular sector S of width $\pi/3$, centered in $(V_i'')^1$ or $(V_i'')^2$, and such that $S \cap G_n = \emptyset$.*
- (ii) *Every hexagon in \mathcal{L} with side $r_{G_n} + 2$ has a corner edge and a corresponding angular sector of width $\pi/3$ which do not intersect G_n .*

Proof. By Proposition 5.5 we can assume that v_0'' does not intersect G_n . Assume first that both $(V_0'')^1$ and $(V_0'')^2$ do not disconnect any zigzag path. Consider the two half zigzag paths in which v_0'' divides s_0'' . Then at least one of them does not intersect G_n . Analogously, at least one of the two half zigzag paths in which v_0' divides s_0' does not intersect G_n . Finally, the two half zigzag paths, departing from $(V_0')^1$ and

22 *Elisa Davoli, Paolo Piovano, and Ulisse Stefanelli*

$(V_0')^2$, not parallel to s_0 and s_5 , and in the opposite direction with respect to the center of H_{G_n} , do not intersect G_n . According to the geometric position of the four half-zigzag paths identified beforehand, and using again the hex-connectedness of G_n we obtain (i), the sector S being of width $2\pi/3$. The case in which at least one between $(V_0'')^1$ and $(V_0'')^2$ disconnects one zigzag path (see Proposition 5.2) follows accordingly, yielding a sector S of width $\pi/3$. The proof of (ii) is an adaptation of the proof of (i). \square

Without loss of generality, in view of Proposition 5.6 we can assume that $v_0'' \notin G_n$. For $k = 2, 3, 4, 5$, let π'_k be the subset of \mathcal{L} such that

$$\begin{cases} \pi'_k = F(\pi'_k) \cap \mathcal{L}, \\ \partial F(\pi'_k) \cap \mathcal{L} = s_k^{\lambda_k}, \\ H_{G_n} \subset \pi'_k. \end{cases}$$

Consider the set $R := \left(\bigcap_{k=0}^5 \pi'_k \right) \setminus H_{G_n}^+$.

By construction, $G_n \subset H_{G_n}^+ \cup R$, and for every $x \in R$ and $k = 0, \dots, 5$ there exists

$$j_k \in \left[-\lambda_{\left(\frac{k+3}{6} - \lfloor \frac{k+3}{6} \rfloor\right)} - 2r_{G_n} - 2, \lambda_k \right]$$

such that $x \in s_k^{j_k}$. In particular, every $x \in R$ is uniquely determined by a pair of indexes $(j_k, j_{k'})$, with $k' \neq k + 3$ in \mathbb{Z}_6 .

We subdivide the region R into disjoint polygons as

$$R = \left(\bigcup_{j=0}^5 P_j \right) \cup \left(\bigcup_{j=0}^5 T_j \right). \quad (5.6)$$

For $a \in [-2(r_{G_n} + 1), 2(r_{G_n} + 1)]$, denote by $P_k^1(a)$ the subset of \mathcal{L} enclosed by s_k^2 , s_k^a , s_{k+1}^1 , $s_{k+1}^{-r_{G_n}}$; and by $P_k^2(a)$ the set delimited by s_k^a , $s_k^{\lambda_k}$, $s_{k-1}^{\lambda_{k-1} - r_{G_n}}$, $s_{k-1}^{\lambda_{k-1}}$. For $k = 0, \dots, 5$, the sets P_k in (5.6) are defined as follows:

$$P_k := \begin{cases} P_k^1(\lambda_k) \cap R & \text{if } \lambda_k \leq \lambda_{k-1} + 1, \\ (P_k^1(\lambda_k - \lambda_{k-1} + 1) \cap R) \cup P_k^2(\lambda_k - \lambda_{k-1} + 1) & \text{if } \lambda_k > \lambda_{k-1} + 1, \end{cases}$$

with the convention that $\lambda_{-1} := \lambda_5$. Note that $|P_k| = 2(r_{G_n} + 1)(\lambda_k - 1)$ for every $k = 0, \dots, 5$.

The sets T_k are given, roughly speaking, by the ‘‘portions of \mathcal{L} ’’ between P_{k-1} and P_k . To be precise,

$$T_k := \left\{ x \in R : x \in s_{k-1}^{j_{k-1}} \cap s_k^{j_k}, \text{ with } 2 \leq j_{k-1} \leq \lambda_{k-1}, 2 \leq j_k \leq \lambda_k, j_{k-1} \geq j_k \right. \\ \left. \text{and, if } \lambda_{k-1} > \lambda_{k-2} + 1, j_{k-1} \leq j_k + \lambda_{k-1} - \lambda_{k-2} \right\}, \quad (5.7)$$

see Figure 7.

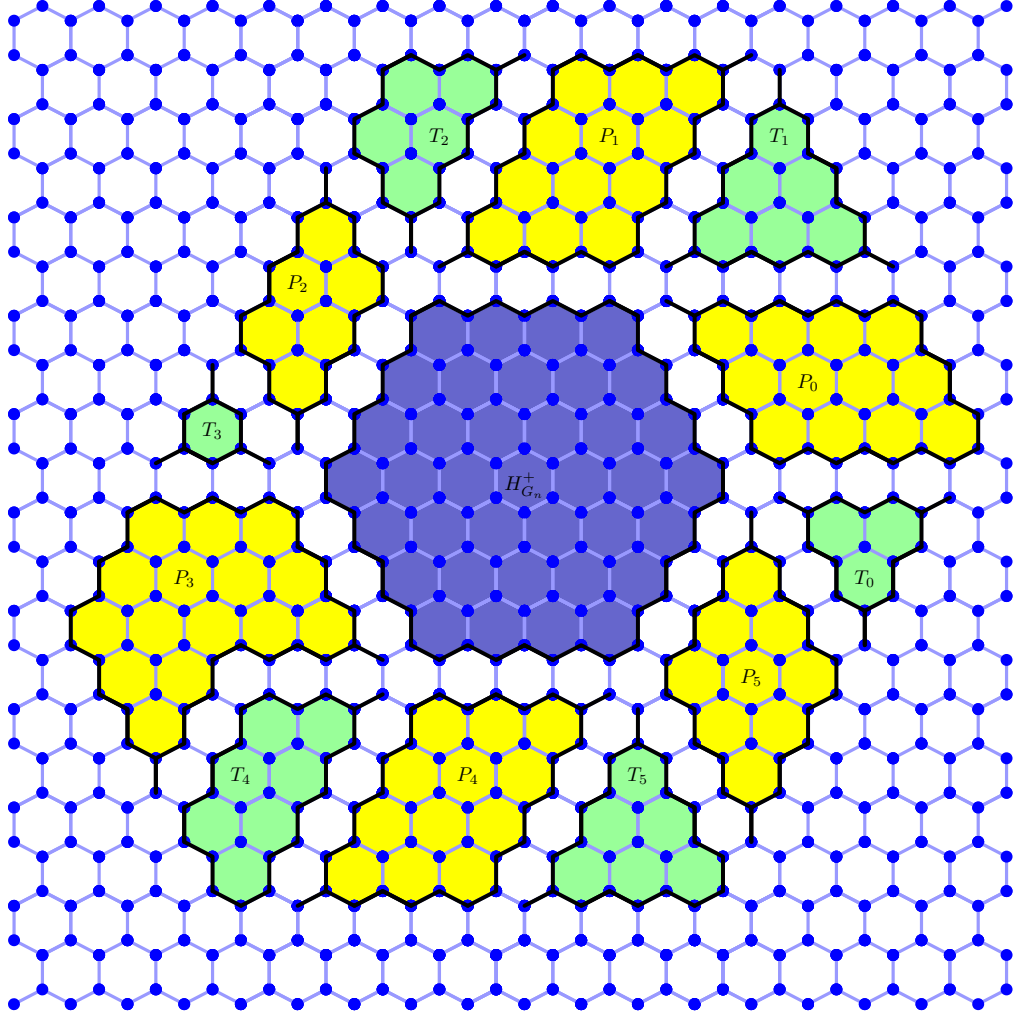


Fig. 7. The structure of a ground state G_n . In the figure above, $r_{G_n} = 3$, $\lambda_0 = 6$, $\lambda_1 = 6$, $\lambda_2 = 4$, $\lambda_3 = 7$, $\lambda_4 = 6$, and $\lambda_5 = 5$. The blue shape outlined in black, the yellow shapes outlined in black, and the green shapes outlined in black correspond to the closed subsets of the plane associated to $H_{G_n}^+$, to the parallelograms P_j , and to the triangles T_j , respectively.

We have that

$$n \leq |H_{G_n}^+| + |R| - |R \setminus G_n|,$$

where $|H_{G_n}^+| = 6(r_{G_n} + 1)^2$. We observe that

$$|R| = \sum_{j=0}^5 |P_j| + \sum_{j=0}^5 |T_j| = 2(r_{G_n} + 1) \sum_{j=0}^5 (\lambda_j - 1) + \sum_{j=0}^5 |T_j| - 1.$$

24 *Elisa Davoli, Paolo Piovano, and Ulisse Stefanelli*

We proceed now in counting the points in R which do not belong to the ground state G_n . In particular, we prove a lower bound for such number in terms of the cardinality of

$$\mathcal{H} := \{H \in \mathcal{L} \cap (H_{G_n}^+ \cup R) : H \text{ is a hexagon of side } r_{G_n} + 2\}.$$

Proposition 5.7.

$$|R \setminus G_n| \geq 2|\mathcal{H}|.$$

Proof. Set $M := |\mathcal{H}|$. We show by induction on $m = 1, \dots, M$ that for every family $\mathcal{H}_m \subset \mathcal{H}$ with $|\mathcal{H}_m| = m$, there exists a collection of pairs of bonded atoms $V_{\mathcal{H}_m} \subset R \setminus G_n$ with $|V_{\mathcal{H}_m}| = m$ satisfying the following property: identifying each segment with its extrema, the correspondence associating to each pair $(\nu_1, \nu_2) \in V_{\mathcal{H}_m}$ a hexagon $H \in \mathcal{H}_m$ having a corner edge in (ν_1, ν_2) is a bijection.

We remark that the thesis will follow once we prove the assertion for $m = M$. For $m = 1$ the claim holds by Proposition 5.6. Assume now that the claim is satisfied for $m = \bar{m}$. Consider a family $\mathcal{H}_{\bar{m}+1} = \{H_1, \dots, H_{\bar{m}+1}\} \subset \mathcal{H}$, and the polygon $\mathcal{P}_{\bar{m}+1} := \cup_{i=1}^{\bar{m}+1} H_i \subset R$. We subdivide the remaining part of the proof into 4 steps.

Step 1: there exists a corner edge $(\tilde{\nu}_1, \tilde{\nu}_2)$ of $\mathcal{P}_{\bar{m}+1}$ such that $\tilde{\nu}_i \in \mathcal{P}_{\bar{m}+1} \setminus G_n$ for $i = 1, 2$.

Indeed, assume by contradiction that every corner edge of $\mathcal{P}_{\bar{m}+1}$ belongs to G_n . Then every corner edge of $H_{\bar{m}+1}$ in $\mathring{F}(\mathcal{P}_{\bar{m}+1})$ would belong to G_n by Proposition 5.3. Thus all corner edges of $H_{\bar{m}+1}$ would belong to G_n , contradicting Proposition 5.5.

Step 2: by Proposition 5.6 (ii) there exists an angular sector S of width at least $\pi/3$, centered in $\tilde{\nu}_1, \tilde{\nu}_2$, or in $(\tilde{\nu}_1, \tilde{\nu}_2)$, and such that $\bar{S} \cap G_n = \emptyset$. Denote by σ_1 and σ_2 the two zigzag paths forming its boundary.

Step 3: We claim that there exists a corner edge (ν_1, ν_2) of $\mathcal{P}_{\bar{m}+1}$ such that $(\nu_1, \nu_2) \subset \mathcal{P}_{\bar{m}+1} \setminus G_n$, and (ν_1, ν_2) is associated to an angle $2\pi/3$ of $\mathcal{P}_{\bar{m}+1}$.

Observe that $\mathcal{P}_{\bar{m}+1}$ can have corner edges with angles $2\pi/3$, $4\pi/3$, or $5\pi/3$. If the corner edge $(\tilde{\nu}_1, \tilde{\nu}_2)$ found in Step 2 is associated to an angle $2\pi/3$, there is nothing to prove. If $(\tilde{\nu}_1, \tilde{\nu}_2)$ corresponds to an angle $4\pi/3$, or $5\pi/3$, then there are two possible cases:

Case 1: $F(\bar{S}) \cap \mathcal{P}_{\bar{m}+1} = \emptyset$. Then, for every $j = 1, 2$, there exists $\hat{\nu}_j \in \sigma_j$ such that $\hat{\nu}_j$ is one of the two extrema of a corner edge of $\mathcal{P}_{\bar{m}+1}$ entirely contained in

S , and at least one among the zigzag paths from $\hat{\nu}_1$ to $\tilde{\nu}_1$ and from $\hat{\nu}_2$ to $\tilde{\nu}_2$ is contained in $\partial F(\mathcal{P}_{\bar{m}+1})$. In addition, the corner edge associated to such $\tilde{\nu}_j$ does not intersect G_n (because it is a subset of S), and is associated to an angle $2\pi/3$ (since $F(\overset{\circ}{S}) \cap \mathcal{P}_{\bar{m}+1} = \emptyset$). The proof follows by considering the corner edge associated to $\hat{\nu}_j$.

Case 2: $F(\overset{\circ}{S}) \cap \mathcal{P}_{\bar{m}+1} \neq \emptyset$. Let ℓ_1 and ℓ_2 be the lines generating σ_1 and σ_2 , and let n_1 and n_2 be the unit normal vectors to ℓ_1 and ℓ_2 , respectively, pointing outside S . Define

$$\sigma_1^k := \sigma_1 - \frac{3}{2}kn_1 \quad \text{and} \quad \sigma_2^k := \sigma_2 - \frac{3}{2}kn_2.$$

for $k \in \mathbb{N}$. Since $\mathcal{P}_{\bar{m}+1} \cap S$ is bounded, we can find

$$k_1 := \max\{k \in \mathbb{N} : \sigma_1^k \cap \mathcal{P}_{\bar{m}+1} \cap S \neq \emptyset\}$$

and

$$k_2 := \max\{k \in \mathbb{N} : \sigma_2^k \cap \mathcal{P}_{\bar{m}+1} \cap S \neq \emptyset\}.$$

For $j = 1, 2$, the intersection $\sigma_j^{k_j} \cap \partial F(\mathcal{P}_{\bar{m}+1}) \cap S$ is either a corner edge of $\mathcal{P}_{\bar{m}+1}$ associated to an angle $2\pi/3$, or a zigzag path forming an angle $2\pi/3$ with a corner edge of $\mathcal{P}_{\bar{m}+1}$.

Step 4: Let (ν_1, ν_2) be the corner edge provided by Step 3. Then, there exists a unique $H_{\bar{j}} \in \mathcal{H}_{\bar{m}+1}$ having a corner edge identified by (ν_1, ν_2) . Thus, by the induction hypothesis on $\{H_1, \dots, H_{\bar{m}+1}\} \setminus \{H_{\bar{j}}\}$, there exists a family of corner edges

$$\{(\nu_1^j, \nu_2^j)\}_{j=1, \dots, \bar{m}+1, j \neq \bar{j}} \subset R \setminus G_n$$

such that, for every j , (ν_1^j, ν_2^j) is a corner edge of H_j , and for every $i \neq j$ (ν_1^j, ν_2^j) is not a corner edge of H_i . The thesis follows by setting $(\nu_1^{\bar{j}}, \nu_2^{\bar{j}}) = (\nu_1, \nu_2)$, and taking $V_{\mathcal{H}_{\bar{m}+1}} = \{(\nu_1^1, \nu_2^1), \dots, (\nu_1^{\bar{m}+1}, \nu_2^{\bar{m}+1})\}$. \square

The next step consists in estimating $|\mathcal{H}|$ from below, in terms of the cardinality of the sets T_j and the number of levels λ_j .

Proposition 5.8.

$$2|\mathcal{H}| \geq \sum_{j=0}^5 |T_j| - 2\lambda_1 - 4\lambda_2 - 4\lambda_3 - 4\lambda_4 - 2\lambda_5 + 18.$$

Proof. For $k = 2, 3, 4, 5$, let U_k be the region of \mathcal{L} containing $H_{G_n}^+$ and delimited by the zigzag paths s_{k+1}^1 , s_{k+2}^1 , and s_{k+3}^1 (with $s_6^1 := s_0^1$, $s_7^1 := s_1^1$, and $s_8^1 := s_2^1$). Let $\mathcal{H}_k := \{H \in \mathcal{H} : H \subset U_k \text{ and has a vertex in } T_k\}$, $k = 2, 3, 4, 5$.

26 *Elisa Davoli, Paolo Piovano, and Ulisse Stefanelli*

We claim that

$$|\mathcal{H}_k| \geq \frac{|T_k| - 2(\lambda_k + \lambda_{k-1} - 3)}{2}. \quad (5.8)$$

Indeed, let $(\tilde{x}, \hat{x}) \in T_k$ and consider $(\tilde{j}_k, \tilde{j}_{k-1}, \tilde{j}_{k-2})$ such that $\tilde{x} \in s_k^{\tilde{j}_k} \cap s_{k-1}^{\tilde{j}_{k-1}} \cap s_{k-2}^{\tilde{j}_{k-2}}$ and $\hat{x} \in s_k^{\tilde{j}_k} \cap s_{k-1}^{\tilde{j}_{k-1}} \cap s_{k-2}^{\tilde{j}_{k-2}-1}$. We identify \tilde{x} and \hat{x} with the triple of indexes $(\tilde{j}_k, \tilde{j}_{k-1}, \tilde{j}_{k-2})$ and $(\tilde{j}_k, \tilde{j}_{k-1}, \tilde{j}_{k-2} - 1)$, and we write $\tilde{x} = (\tilde{j}_k, \tilde{j}_{k-1}, \tilde{j}_{k-2})$ and $\hat{x} = (\tilde{j}_k, \tilde{j}_{k-1}, \tilde{j}_{k-2} - 1)$. Let $H_{\tilde{x}, \hat{x}}$ be the hexagon with corner edges identified by the pairs (\tilde{x}, \hat{x}) , and the pairs

$$\begin{aligned} w_1 &:= [(\tilde{j}_k - (r_{G_n} + 2), \tilde{j}_{k-1}, \tilde{j}_{k-2} + (r_{G_n} + 1)), (\tilde{j}_k - (r_{G_n} + 1), \tilde{j}_{k-1}, \tilde{j}_{k-2} + (r_{G_n} + 1))] \\ w_2 &:= [(\tilde{j}_k - (2r_{G_n} + 3), \tilde{j}_{k-1} - (r_{G_n} + 2), \tilde{j}_{k-2} + (r_{G_n} + 1)), \\ &\quad (\tilde{j}_k - (2r_{G_n} + 3), \tilde{j}_{k-1} - (r_{G_n} + 1), \tilde{j}_{k-2} + (r_{G_n} + 1))], \\ w_3 &:= [(\tilde{j}_k - (2r_{G_n} + 3), \tilde{j}_{k-1} - (2r_{G_n} + 3), \tilde{j}_{k-2} - 1), \\ &\quad (\tilde{j}_k - (2r_{G_n} + 3), \tilde{j}_{k-1} - (2r_{G_n} + 3), \tilde{j}_{k-2})], \\ w_4 &:= [(\tilde{j}_k - (r_{G_n} + 1), \tilde{j}_{k-1} - (2r_{G_n} + 3), \tilde{j}_{k-2} - (r_{G_n} + 2)), \\ &\quad (\tilde{j}_k - (r_{G_n} + 2), \tilde{j}_{k-1} - (2r_{G_n} + 3), \tilde{j}_{k-2} - (r_{G_n} + 2))], \\ w_5 &:= [(\tilde{j}_k, \tilde{j}_{k-1} - (r_{G_n} + 2), \tilde{j}_{k-2} - (r_{G_n} + 2)), (\tilde{j}_k, \tilde{j}_{k-1} - (r_{G_n} + 1), \tilde{j}_{k-2} - (r_{G_n} + 2))]. \end{aligned}$$

We observe that $H_{\tilde{x}, \hat{x}}$ is contained in U_k and has a corner edge in T_k if the following inequalities are satisfied

$$\begin{aligned} \tilde{j}_k - (2r_{G_n} + 3) &\geq -2r_{G_n} - 1, & \tilde{j}_k &\leq \lambda_k, \\ \tilde{j}_{k-1} - (2r_{G_n} + 3) &\geq -2r_{G_n} - 1, & \tilde{j}_{k-1} &\leq \lambda_{k-1}, \\ \tilde{j}_{k-2} - (r_{G_n} + 2) &\geq -2r_{G_n} - 1, & \tilde{j}_{k-2} + r_{G_n} + 1 &\leq \lambda_{k-2}. \end{aligned}$$

Hence, if $(\tilde{j}_k, \tilde{j}_{k-1}, \tilde{j}_{k-2})$ is such that

$$\begin{aligned} 2 &\leq \tilde{j}_k \leq \lambda_k, \\ 2 &\leq \tilde{j}_{k-1} \leq \lambda_{k-1}, \\ -r_{G_n} + 1 &\leq \tilde{j}_{k-2} \leq \lambda_{k-2} - r_{G_n} - 1, \end{aligned}$$

then $H_{\tilde{x}, \hat{x}} \subset U_k$ and has a corner edge in T_k . By the definition of the sets T_k (see (5.7)), the previous properties are fulfilled by every $x \in T_k$, apart from those points belonging to the portion of $\partial F(T_k)$ which is adjacent either to P_{k-1} or to P_k . Denoting by \tilde{T}_k this latter set, claim (5.8) follows once we observe that

$$|\tilde{T}_k| = \frac{|T_k| - 2(\lambda_k + \lambda_{k-1} - 3)}{2}. \quad \square$$

Combining Propositions 5.7 and 5.8 we estimate from above and from below the radius r_{G_n} of the maximal hexagon H_{G_n} .

Proposition 5.9.

$$\rho_n \leq r_n \leq R_n \leq \rho_n + \frac{2}{3} \sqrt{[(\alpha_n)^2 - [(\alpha_n)^2 - \alpha_n]^2 - (\alpha_n)^2 + 39]},$$

where

r_n is the quantity defined in (1.6), $R_n := \max\{r_{G_n} : G_n \text{ is a ground state with } n \text{ atoms}\}$, and

$$\rho_n := \frac{(\alpha_n)^2}{3} - \frac{\lfloor (\alpha_n)^2 - \alpha_n \rfloor}{3} - 3 - \frac{1}{3} \sqrt{[(\alpha_n)^2 - \lfloor (\alpha_n)^2 - \alpha_n \rfloor]^2 - (\alpha_n)^2 + 39}, \quad (5.9)$$

with $\alpha_n = \sqrt{3n/2}$.

Proof. By Propositions 5.7 and 5.8 we have

$$|R \setminus G_n| \geq \sum_{j=0}^5 |T_j| - 2\lambda_1 - 4\lambda_2 - 4\lambda_3 - 4\lambda_4 - 2\lambda_5 + 18.$$

Therefore, by (5.3) we obtain

$$\begin{aligned} n &\leq |H_{G_n}^+| + |R| - |R \setminus G_n| \\ &\leq 6(r_{G_n} + 1)^2 + \sum_{j=0}^5 |P_j| + \sum_{j=0}^5 |T_j| - \sum_{j=0}^5 |T_j| + 2\lambda_1 + 4\lambda_2 + 4\lambda_3 + 4\lambda_4 + 2\lambda_5 - 18 \\ &\leq 6(r_{G_n} + 1)^2 + (2r_{G_n} + 6) \left(\sum_{k=0}^5 \lambda_k - 1 \right) + 2 \\ &= 6(r_{G_n} + 1)^2 + (r_{G_n} + 3)(p_n - 12r_{G_n} - 6) + 2 \\ &= -6(r_{G_n} + 1)^2 + (p_n - 18)(r_{G_n} + 1) + 2p_n + 14. \end{aligned}$$

The thesis follows by solving the inequality with respect to $r_{G_n} + 1$ and using the definitions of r_n , p_n and α_n (see Proposition 3.4). \square

We conclude this section with a refinement of the estimate from above on r_n .

Proposition 5.10.

$$r_n \leq \rho_n + O(1).$$

Proof. For every $n \in \mathbb{N}$, $n > 6$, let

$$\tilde{\rho}_n := \left\lceil \frac{(\alpha_n)^2}{3} - \frac{\lfloor (\alpha_n)^2 - \alpha_n \rfloor}{3} - \frac{1}{3} \sqrt{[(\alpha_n)^2 - \lfloor (\alpha_n)^2 - \alpha_n \rfloor]^2 - (\alpha_n)^2} \right\rceil. \quad (5.10)$$

Let $H_{\tilde{\rho}_n} := D_{6\tilde{\rho}_n^2}$, and

$$h_n := \frac{p_n - P(H_{\tilde{\rho}_n})}{4} = \frac{p_n - 6(2\tilde{\rho}_n - 1)}{4} = \frac{p_n}{4} - 3\tilde{\rho}_n + \frac{3}{2}.$$

Consider the hexagonal configurations C_c given by the union of the hexagons $H_{\tilde{\rho}_n}$ with the “parallelograms” of height h_n constructed on two consecutive sides of $H_{\tilde{\rho}_n}$.

28 *Elisa Davoli, Paolo Piovano, and Ulisse Stefanelli*

To be precise, denoting by s_0^n, \dots, s_5^n the zigzag paths passing through the sides of $H_{\tilde{\rho}_n}$, and setting

$$s_k^{n,j} := s_k^n + j\mathbf{e}_k, \quad k = 0, \dots, 5,$$

for every $n \in \mathbb{N}$, define the set C_c to be the portion of \mathcal{L} enclosed by the zigzag paths $s_0^n, s_1^{n,h_n}, s_2^{n,h_n}, s_3^n, s_4^n, s_5^n$.

By construction, the perimeter of C_c satisfies

$$P(C_c) = p_n.$$

We claim that for n big enough there exists a ground state G_n such that $H_{\tilde{\rho}_n} \subseteq G_n \subseteq C_c$, and $|C_c \setminus G_n| \leq 2\tilde{\rho}_n - 1$. Indeed,

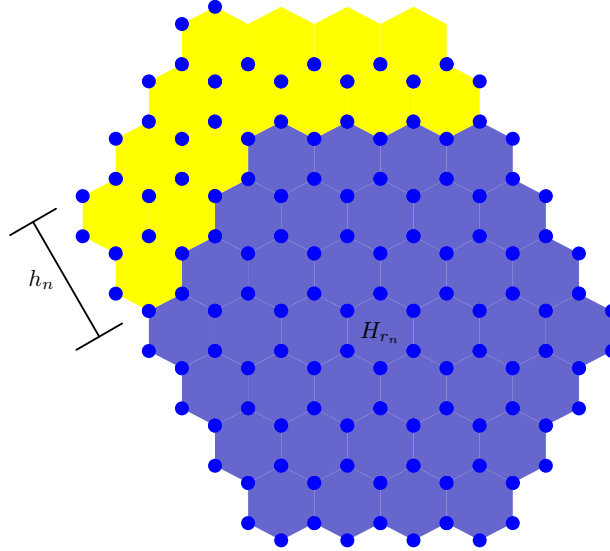


Fig. 8. In the figure above, $n = 120$, $\tilde{\rho}_n = 4$ and $h_n = 2$. The configuration C_c is defined as the union of $H_{\tilde{\rho}_n}$ with the two yellow parallelograms of height h_n , constructed on the sides of $H_{\tilde{\rho}_n}$. The ground state G_n (given by the collection of the blue atoms) satisfies $H_{\tilde{\rho}_n} \subseteq G_n \subseteq C_c$, and $|C_c \setminus G_n| \leq 2\tilde{\rho}_n - 1$.

$$\begin{aligned} |C_c| &= |H_{\tilde{\rho}_n}| + 4\tilde{\rho}_n h_n = 6\tilde{\rho}_n^2 + \tilde{\rho}_n [p_n - 6(2\tilde{\rho}_n - 1)] \\ &= -6\tilde{\rho}_n^2 + (p_n + 6)\tilde{\rho}_n. \end{aligned} \quad (5.11)$$

A direct computation shows that

$$6s^2 - (p_n + 6)s + n \leq 0$$

for every s satisfying

$$s \in \left[\frac{(\alpha_n)^2}{3} - \frac{[(\alpha_n)^2 - \alpha_n]}{3} - \frac{1}{3} \sqrt{[(\alpha_n)^2 - [(\alpha_n)^2 - \alpha_n]]^2 - (\alpha_n)^2}, \right.$$

$$\frac{(\alpha_n)^2}{3} - \frac{[(\alpha_n)^2 - \alpha_n]}{3} + \frac{1}{3} \sqrt{[(\alpha_n)^2 - [(\alpha_n)^2 - \alpha_n]]^2 - (\alpha_n)^2}, \quad (5.12)$$

whereas

$$6s^2 - (4 + p_n)s + n - 1 \geq 0$$

for every $s \in \mathbb{R}$ such that

$$s \leq -\frac{1}{6} + \frac{(\alpha_n)^2}{3} - \frac{[(\alpha_n)^2 - \alpha_n]}{3} - \frac{1}{3} \sqrt{[(\alpha_n)^2 - [(\alpha_n)^2 - \alpha_n]]^2 - (\alpha_n)^2 - \frac{1}{4} - p_n}$$

or

$$s \geq -\frac{1}{6} + \frac{(\alpha_n)^2}{3} - \frac{[(\alpha_n)^2 - \alpha_n]}{3} + \frac{1}{3} \sqrt{[(\alpha_n)^2 - [(\alpha_n)^2 - \alpha_n]]^2 - (\alpha_n)^2 - \frac{1}{4} - p_n}. \quad (5.13)$$

In particular, (5.12) and (5.13) hold for $s = \tilde{\rho}_n$, yielding

$$0 \leq |C_c| - n \leq 2\tilde{\rho}_n - 1. \quad (5.14)$$

The claim follows by (5.14), and by observing that by the definition of C_c it is possible to remove up to $2\tilde{\rho}_n - 1$ points from $C_c \setminus H_{\tilde{\rho}_n}$ without changing the perimeter of the configuration. In particular, $H_{G_n} = H_{\tilde{\rho}_n}$. The thesis is thus a direct consequence of (1.6), (5.9), and (5.10). \square

6. Sharp convergence to the Wulff shape

In this section we prove that as the number n of atoms tends to infinity, ground states differ from a hexagonal Wulff shape by at most $O(n^{3/4})$ points and we show that this estimate is sharp. The proof strategy consists in exploiting Proposition 5.9 to deduce an upper bound on the number of points belonging to G_n but not to the n -Wulff shape W_n .

Let W be the regular hexagon defined as the convex hull of the vectors

$$\left\{ \pm \frac{1}{\sqrt{6}} t_1, \pm \frac{1}{\sqrt{6}} t_2, \pm \frac{1}{\sqrt{6}} (t_2 - t_1) \right\},$$

and let χ_W be its characteristic function. Denote by μ the measure

$$\mu := \frac{4}{\sqrt{3}} \chi_W.$$

30 *Elisa Davoli, Paolo Piovano, and Ulisse Stefanelli*

6.1. Proof of Theorem 1.2

We subdivide the proof into two steps.

Step 1: Let G_n be a ground state. Without loss of generality, assume that $n > 6$, and hence, by Proposition 5.1, that the maximal hexagon H_{G_n} is not degenerate and $r_n \geq 1$. Let $q_n \in \mathcal{L}$ be such that $H_{G_n} = D_{6r_{G_n}^2} + q_n$. We claim that

$$d_{\mathcal{H}}(G'_n, W_n) \leq O(n^{1/4}), \quad (6.1)$$

and

$$|G'_n \setminus W_n| = K_n n^{3/4} + o(n^{3/4}), \quad (6.2)$$

where

$$G'_n := G_n - q_n,$$

and

$$K_n := \frac{4\alpha_n}{3n^{3/4}} \sqrt{((\alpha_n)^2 - [(\alpha_n)^2 - \alpha_n])^2 - (\alpha_n)^2}, \quad (6.3)$$

with $\alpha_n = \sqrt{3n/2}$.

Indeed, we first observe that

$$d_{\mathcal{H}}(G_n, H_{G_n}) \leq \max_{i=0,\dots,5} \lambda_i.$$

In view of (5.3) and of Proposition 5.9, we obtain the upper bounds

$$\begin{aligned} d_{\mathcal{H}}(G_n, H_{G_n}) &\leq 2(\alpha_n^2) - 2[(\alpha_n)^2 - \alpha_n] - 6\rho_n \\ &\leq 18 + 2\sqrt{[(\alpha_n)^2 - [(\alpha_n)^2 - \alpha_n]]^2 - (\alpha_n)^2 + 39}, \end{aligned}$$

and

$$d_{\mathcal{H}}(H_{G'_n}, W_n) \leq r_{G_n} - r_n \leq \frac{2}{3} \sqrt{[(\alpha_n)^2 - [(\alpha_n)^2 - \alpha_n]]^2 - (\alpha_n)^2 + 39}.$$

On the other hand, Propositions 5.9 and 5.10 yield the equality

$$\begin{aligned} |G'_n \setminus W_n| &= n - 6r_n^2 \\ &= n - 6\rho_n^2 - 6(r_n + \rho_n)(r_n - \rho_n) \\ &= n - 6\rho_n^2 + O(n^{1/2}) \\ &= n - 6\left(\frac{\alpha_n}{3} + \frac{(\alpha_n)^2 - \alpha_n}{3} - \frac{[(\alpha_n)^2 - \alpha_n]}{3} - 3\right. \\ &\quad \left. - \frac{1}{3} \sqrt{[(\alpha_n)^2 - [(\alpha_n)^2 - \alpha_n]]^2 - (\alpha_n)^2 + 39}\right)^2 + o(n^{3/4}) \\ &= n - 6\left(\frac{(\alpha_n)^2}{9} - \frac{2\alpha_n}{9} \sqrt{[(\alpha_n)^2 - [(\alpha_n)^2 - \alpha_n]]^2 - (\alpha_n)^2 + 39}\right) + o(n^{3/4}) \\ &= \frac{4\alpha_n}{3} \sqrt{[(\alpha_n)^2 - [(\alpha_n)^2 - \alpha_n]]^2 - (\alpha_n)^2} + o(n^{3/4}). \end{aligned} \quad (6.4)$$

Claims (6.1) and (6.2) follow now by the definition of α_n and by the observation that

$$\sqrt{[(\alpha_n)^2 - \lfloor(\alpha_n)^2 - \alpha_n\rfloor]^2 - (\alpha_n)^2} = \sqrt{2\eta_n\alpha_n + \eta_n^2} \leq 1 + \sqrt{\alpha_n} = O(n^{1/4}),$$

where $\eta_n := (\alpha_n)^2 - \alpha_n - \lfloor(\alpha_n)^2 - \alpha_n\rfloor$.

Step 2: Step 1 yields the equality

$$\|\mu_{G'_n} - \mu_{W_n}\| = \frac{|G'_n \Delta W_n|}{n} = K_n n^{-1/4} + o(n^{-1/4}), \quad (6.5)$$

where $\mu_{G'_n}$ and μ_{W_n} are the empirical measures associated to G'_n and W_n , respectively (see (2.3)). Let $\mu_n := \mu_{W_n}$.

For every $x_i \in W_n$, denote by Ω_i its Voronoi cell in \mathcal{L} , that is the equilateral triangle centered in x_i , of side $\sqrt{3}$ and with edges orthogonal to the three lattice directions. Finally, define Ω_i^n as the set

$$\Omega_i^n := \{x/\sqrt{n} : x \in \Omega_i\}.$$

Let $\varphi \in W^{1,\infty}(\mathbb{R}^2)$. We observe that

$$\left\| \frac{x_i}{\sqrt{n}} - x \right\|_{L^\infty(\Omega_i^n)} \leq \sqrt{\frac{3}{n}},$$

and by (6.4),

$$\begin{aligned} \mathcal{L}^2\left(\left(\cup_{i=1}^{6r_n^2} \Omega_i^n\right) \Delta W\right) &= \left| \frac{3\sqrt{3}}{2} \left(\frac{\sqrt{3}r_n}{\sqrt{n}}\right)^2 - \frac{3\sqrt{3}}{4} \right| = \frac{3\sqrt{3}}{4} \left| \frac{6r_n^2}{n} - 1 \right| \\ &= \frac{3\sqrt{3}}{4} \left| \frac{n - K_n n^{3/4}}{n} - 1 \right| = \frac{3\sqrt{3}}{4} K_n n^{-1/4}. \end{aligned}$$

Thus, we obtain

$$\begin{aligned} \left| \int_{\mathbb{R}^2} \varphi d\mu_n - \int_{\mathbb{R}^2} \varphi d\mu \right| &= \left| \frac{1}{n} \sum_{i=1}^{6r_n^2} \varphi\left(\frac{x_i}{\sqrt{n}}\right) - \frac{4}{3\sqrt{3}} \int_W \varphi dx \right| \quad (6.6) \\ &= \frac{4}{3\sqrt{3}} \left| \sum_{i=1}^{6r_n^2} \varphi\left(\frac{x_i}{\sqrt{n}}\right) \mathcal{L}^2(\Omega_i^n) - \int_W \varphi dx \right| \\ &\leq \frac{4}{3\sqrt{3}} \left| \sum_{i=1}^{6r_n^2} \int_{\Omega_i^n} \left(\varphi\left(\frac{x_i}{\sqrt{n}}\right) - \varphi(x)\right) dx \right| + \frac{4}{3\sqrt{3}} \|\varphi\|_{L^\infty(\mathbb{R}^2)} \mathcal{L}^2\left(\left(\cup_{i=1}^{6r_n^2} \Omega_i^n\right) \Delta W\right) \\ &\leq \frac{4}{3\sqrt{3}} \|\nabla\varphi\|_{L^\infty(\mathbb{R}^2;\mathbb{R}^2)} \sum_{i=1}^{6r_n^2} \int_{\Omega_i^n} \left| \frac{x_i}{\sqrt{n}} - x \right| dx + \frac{4}{3\sqrt{3}} \|\varphi\|_{L^\infty(\mathbb{R}^2)} \mathcal{L}^2\left(\left(\cup_{i=1}^{6r_n^2} \Omega_i^n\right) \Delta W\right) \\ &\leq \frac{4}{3\sqrt{n}} \|\nabla\varphi\|_{L^\infty(\mathbb{R}^2;\mathbb{R}^2)} \mathcal{L}^2\left(\cup_{i=1}^{6r_n^2} \Omega_i^n\right) + \frac{4}{3\sqrt{3}} \|\varphi\|_{L^\infty(\mathbb{R}^2)} \mathcal{L}^2\left(\left(\cup_{i=1}^{6r_n^2} \Omega_i^n\right) \Delta W\right) \\ &= \|\varphi\|_{W^{1,\infty}(\mathbb{R}^2)} o(n^{-1/4}) + \|\varphi\|_{L^\infty(\mathbb{R}^2)} K_n n^{-1/4}. \end{aligned}$$

32 *Elisa Davoli, Paolo Piovano, and Ulisse Stefanelli*

Denoting by G'_n the set $G'_n := G_n - q_n$, and by $\mu_{G'_n}$ its associated empirical measure, inequalities (6.5) and (6.6) yield

$$\mu_{(G_n)'} \rightharpoonup^* \mu, \quad \text{weakly* in } M_b(\mathbb{R}^2), \quad (6.7)$$

and

$$\|\mu_{(G_n)'} - \mu\|_F \leq 2K_n n^{-1/4} + o(n^{-1/4}). \quad (6.8)$$

We notice that $K_n = 0$ for every $n \in \mathbb{N}$ such that $n = 6k^2$ for some $k \in \mathbb{N}$. This reflects the fact that for those n the daisy D_n is the unique ground state, whose maximal hexagon is the daisy itself.

In view of the definition of α_n , a direct computation shows that

$$K_n = \frac{2^{7/4}}{3^{1/4}} \sqrt{\left(\frac{3n}{2} - \sqrt{\frac{3n}{2}}\right) - \left(\left\lfloor \frac{3n}{2} - \sqrt{\frac{3n}{2}} \right\rfloor\right)} + o(1).$$

Hence, in particular,

$$\limsup_{n \rightarrow +\infty} K_n \leq \frac{2^{7/4}}{3^{1/4}} = K.$$

This completes the proof of Theorem 1.2. \square

6.2. Proof of Theorem 1.3

The proof consists in finding a sequence $\{n_i\}$, $i \in \mathbb{N}$, such that

$$K_{n_i} \rightarrow K \quad (6.9)$$

as $i \rightarrow +\infty$. Indeed, in view of (6.2), (6.5), (6.8), (6.9), for every $\{n_i\}$ verifying (6.9), and for every sequence of ground states $\{G_{n_i}\}$, there exist suitable translations $\{G'_{n_i}\}$ such that

$$|G'_{n_i} \setminus W_{n_i}| = Kn_i^{3/4} + o(n_i^{3/4}),$$

$$\|\mu_{G'_{n_i}} - \mu_{W_{n_i}}\| = Kn_i^{-1/4} + o(n_i^{-1/4}),$$

and

$$\|\mu_{G'_{n_i}} - \mu_{W_{n_i}}\|_F = Kn_i^{-1/4} + o(n_i^{-1/4}).$$

A possible choice is to consider

$$n_i := 2 + 6i^2.$$

In fact we have

$$\frac{3n_i}{2} - \sqrt{\frac{3n_i}{2}} = 9i^2 + 3 - \sqrt{9i^2 + 3} = 9i^2 + 3 - 3i - \frac{1}{i\left(1 + \sqrt{1 + \frac{1}{3i^2}}\right)},$$

and hence

$$\left(\frac{3n_i}{2} - \sqrt{\frac{3n_i}{2}}\right) - \left[\left(\frac{3n_i}{2} - \sqrt{\frac{3n_i}{2}}\right)\right] = 1 - \frac{1}{i\left(1 + \sqrt{1 + \frac{1}{3i^2}}\right)} \rightarrow 1$$

as $i \rightarrow +\infty$, which in turn yields (6.9). This completes the proof of Theorem 1.3. \square

Before closing this section let us comment on the fact that, as a byproduct of our construction, we also obtain sharp estimates on the distance of any sequence $\{G_n\}$ of (translated) ground states from the n -Wulff shape, in terms of the constant K_n defined in (6.3) (see (6.2), (6.5), and (6.8)). Let us finally stress the nonuniqueness of the n -dimensional Wulff shape W_n : any zigzag hexagon $D_{6\tilde{r}_n}$, with radius $\tilde{r}_n = r_n + O(1)$ (e.g. $\tilde{r}_n = \tilde{\rho}_n$) would infact lead to the same sharp results.

Acknowledgements

The authors were supported by the Austrian Science Fund (FWF) project P 27052-N25. This work has been funded by the Vienna Science and Technology Fund (WWTF) through project MA14-009. Partial support by the Wolfgang Pauli Institute under the thematic project *Crystals, Polymers, Materials* is also acknowledged. E.D. and P.P. thank the Center for Nonlinear Analysis (NSF Grant No. DMS-0635983), where part of this research was carried out. E.D. was partially funded by the National Science Foundation (NSF) under Grant No. DMS-0905778, and under the PIRE Grant No. OISE-0967140. E.D. is a member of the INdAM-GNAMPA Project 2015 *Critical phenomena in the mechanics of materials: a variational approach*.

References

1. V. Artyukhov, Y. Hao, R.S. Ruoff, B.I. Yakobson, Breaking of symmetry in graphene growth on metal substrates, *Phys. Rev. Lett.* **114** (2015) 115502.
2. Y. Au Yeung, G. Friesecke, B. Schmidt, Minimizing atomic configurations of short range pair potentials in two dimensions: crystallization in the Wulff-shape, *Calc. Var. Partial Differential Equations* **44** (2012) 81–100.
3. L. Barletti, Hydrodynamic equations for electrons in graphene obtained from the maximum entropy principle, *J. Math. Phys.* **55** (2014) 083303.
4. X. Blanc, M. Lewin, The crystallization conjecture: a review, *EMS Surv. Math. Sci.* **2** (2015) 255–306.

34 *Elisa Davoli, Paolo Piovano, and Ulisse Stefanelli*

5. P.S. Branicio, M.H. Jhon, C.K. Gan, D.J. Srolovitz, Properties on the edge: graphene edge energies, edge stresses, edge warping, and the Wulff shape of graphene flakes, *Modelling Simul. Mater. Sci. Eng.* **19** (2011) 054002.
6. V.D. Camiola, V. Romano, Hydrodynamical model for charge transport in graphene, *J. Stat. Phys.* **157** (2014) 1114–1137.
7. G. Dal Maso, *An introduction to Γ -convergence*, Boston, Birkhäuser, 1993.
8. C. Davini, Homogenization of a graphene sheet, *Contin. Mech. Thermodyn.* **26** (2014) 95–113.
9. E. Davoli, P. Piovano, U. Stefanelli, Sharp $n^{3/4}$ law for the minimizers of the edge-isoperimetric problem on the triangular lattice, Submitted (2015).
10. A. Dobry, O. Fojón, M. Gadella, L.P. Lara, Some numerical estimations of energy levels on a model for a graphene ribbon in a magnetic field, *Appl. Math. Comput.* **235** (2014) 8–16.
11. C.T.J. Dodson, A model for gaussian perturbations of graphene, *J. Stat. Phys.* **161** (2015) 933–941.
12. W. E, D. Li, On the crystallization of 2D hexagonal lattices, *Comm. Math. Phys.* **286** (2009) 1099–1140.
13. R. El Hajj, F. Méhats, Analysis of models for quantum transport of electrons in graphene layers, *Math. Models Methods Appl. Sci.* **24** (2014) 2287–2310.
14. D. El Kass, R. Monneau, Atomic to continuum passage for nanotubes: a discrete Saint-Venant principle and error estimates, *Arch. Ration. Mech. Anal.* **213** (2014) 25–128.
15. B. Farmer, S. Esedoğlu, P. Smereka, Crystallization for a Brenner-like potential, *Comm. Math. Phys.*, to appear.
16. C.L. Fefferman, M.I. Weinstein, Wave packets in honeycomb structures and two-dimensional Dirac equations, *Comm. Math. Phys.* **326** (2014) 251–286.
17. L. Flatley, M. Taylor, A. Tarasov, F. Theil, Packing twelve spherical caps to maximize tangencies, *J. Comput. Appl. Math.* **254** (2013) 220–225.
18. L. Flatley, F. Theil, Face-centered cubic crystallization of atomistic configurations, *Arch. Ration. Mech. Anal.* **218** (2015) 363–416.
19. C.K. Gan, D.J. Srolovitz, First-principles study of graphene edge properties and flake shapes, *Phys. Rev. B*, **81** (2010) 125445–125453.
20. C.S. Gardner, C. Radin, The infinite-volume ground state of the Lennard-Jones potential, *J. Stat. Phys.* **20** (1979) 719–724.
21. C.O. Girit, J.C. Meyer, R. Erni, M.D. Rossel, C. Kisielowski, L. Yang, C.H. Park, M.F. Crommie, M.L. Cohen, S.G. Louie, A. Zettl, Graphene at the edge: stability and dynamics, *Science* **27** (2009) 1705–1708.
22. J.E. Graver, C. Graves, S.J. Graves, Fullerene patches II, *Ars Math. Contemp.* **7** (2014) 405–421.
23. L. H. Harper, *Global methods for combinatorial isoperimetric problems*, Cambridge Studies in Advanced Mathematics **90**. Cambridge University Press, Cambridge, 2004.
24. R. Heitmann, C. Radin, Ground states for sticky disks, *J. Stat. Phys.* **22** (1980) 281–287.
25. P. Kerdelhué, J. Royo-Letelier, On the low lying spectrum of the magnetic Schrödinger operator with Kagomé periodicity, *Rev. Math. Phys.* **26** (2014) 1450020, 46.
26. Z. Luo, S. Kim, N. Kawamoto, A.M. Rappe, A.T. Charlie Johnson, Growth mechanism of hexagonal-shape graphene flakes with zigzag edges, *ACS Nano*, **11** (2011) 1954–1960.
27. J. Lu, V. Moroz, C.B. Muratov, Orbital-free density functional theory of out-of-plane charge screening in graphene, *J. Nonlinear Sci.* **25** (2015) 1391–1430.
28. E. Mainini, H. Murakawa, P. Piovano, U. Stefanelli, A numerical investigation on

- carbon-nanotube geometries, *Discrete Contin. Dyn. Syst. - S* (2015), to appear.
29. E. Mainini, H. Murakawa, P. Piovano, U. Stefanelli, Variational modeling of carbon nanotubes, In preparation, 2016.
 30. E. Mainini, P. Piovano, U. Stefanelli, Finite crystallization in the square lattice, *Nonlinearity* **27** (2014) 717–737.
 31. E. Mainini, P. Piovano, U. Stefanelli, Crystalline and isoperimetric square configurations, *Proc. Appl. Math. Mech.* **14** (2014) 1045–1048.
 32. E. Mainini, U. Stefanelli, Crystallization in carbon nanostructures, *Comm. Math. Phys.* **328** (2014) 545–571.
 33. M. Makwana, R.V. Craster, Homogenisation for hexagonal lattices and honeycomb structures, *Quart. J. Mech. Appl. Math.* **67** (2014) 599–630.
 34. D. Monaco, G. Panati, Topological invariants of eigenvalue intersections and decrease of Wannier functions in graphene, *J. Stat. Phys.* **155** (2014) 1027–1071.
 35. D. Monaco, G. Panati, Symmetry and localization in periodic crystals: triviality of Bloch bundles with a fermionic time-reversal symmetry, *Acta Appl. Math.* **137** (2015) 185–203.
 36. C. Radin, The ground state for soft disks, *J. Stat. Phys.* **26** (1981) 365–373.
 37. B. Schmidt, Ground states of the 2D sticky disc model: fine properties and $N^{3/4}$ law for the deviation from the asymptotic Wulff-shape, *J. Stat. Phys.* **153** (2013) 727–738.
 38. F.H. Stillinger, T.A. Weber, Computer simulation of local order in condensed phases of silicon, *Phys. Rev. B* **8** (1985) 5262–5271.
 39. J. Tersoff, New empirical approach for the structure and energy of covalent systems, *Phys. Rev. B* **37** (1988) 6991–7000.
 40. F. Theil, A proof of crystallization in two dimensions, *Comm. Math. Phys.* **262** (2006) 209–236.
 41. W.J. Ventevogel, On the configuration of a one-dimensional system of interacting atoms with minimum potential energy per atom, *Phys. A* **92** (1978) 343–361.
 42. W.J. Ventevogel, B.R.A. Nijboer, On the configuration of systems of interacting atom with minimum potential energy per atom, *Phys. A* **99** (1979) 565–580.
 43. H.J. Wagner, Crystallinity in two dimensions: a note on a paper of C. Radin, *J. Stat. Phys.* **33** (1983) 523–526.
 44. Y. Zhang, L.W. Zhang, K.M. Liew, J.L. Yu, Transient analysis of single-layered graphene sheet using the kp-Ritz method and nonlocal elasticity theory, *Appl. Math. Comput.* **258** (2015) 489–501.